

C and N Abundances in Stars At the Base of the Red Giant Branch in M5 ¹

Judith G. Cohen², Michael M. Briley³ and Peter B. Stetson^{4,5,6}

ABSTRACT

We present an analysis of a large sample of moderate resolution Keck LRIS spectra of subgiant ($V \sim 17.2$) and fainter stars in the Galactic globular cluster M5 (NGC 5904) with the goal of deriving C and N abundances. Star-to-star stochastic variations with significant range in both [C/Fe] and [N/Fe] are found at all luminosities extending to the bottom of the RGB at $M_V \sim +3$. Similar variations in CH appear to be present in the main sequence turnoff spectra, but the signal in the current sample is too low for a detailed analysis. The variations seen among the M5 subgiants are consistent with the abundances found earlier by Briley *et al.* (1992) for brighter giants in this cluster. There is thus no sign of a change in the behavior of C and N with evolutionary stage over the full range in luminosity of the RGB and SGB, although a systematic decrease with luminosity in the mean [C/H] smaller than a factor of 2 cannot be ruled out with confidence at present.

The C and N abundances appear strongly anti-correlated, as would be expected from the CN-cycle processing of stellar material. Yet the present stars are considerably fainter than the RGB bump, the point at which deep mixing is believed to set in. On this basis, while the observed abundance pattern is consistent with proton capture nucleosynthesis, we infer that the site of the reactions is likely not within the present sample, but rather in a population of more massive ($2 - 5M_{\odot}$) now defunct stars.

The range of variation of the N abundances is very large and the sum of C+N increases as C decreases. To reproduce this requires the incorporation not only of CN but also of ON-processed material. Furthermore, the existence of this correlation is quite difficult to reproduce with an external mechanism such as “pollution” with

¹Based on observations obtained at the W.M. Keck Observatory, which is operated jointly by the California Institute of Technology, the University of California and the National Aeronautics and Space Administration

²Palomar Observatory, Mail Stop 105-24, California Institute of Technology, Pasadena, California 91125 (jlc@astro.caltech.edu)

³Department of Physics and Astronomy, University of Wisconsin Oshkosh, Oshkosh, Wisconsin (mike@maxwell.phys.uwosh.edu)

⁴Dominion Astrophysical Observatory, 5071 West Saanich Road, Victoria, British Columbia V9E 2E7 Canada (Peter.Stetson@hia.nrc.ca)

⁵Guest User, Canadian Astronomy Data Centre, which is operated by the Herzberg Institute of Astrophysics, National Research Council of Canada

⁶Guest Investigator at the UK Astronomy Data Centre

material processed in a more massive AGB star, which mechanism is fundamentally stochastic in nature. We therefore suggest that although the internal mixing hypothesis has serious flaws, new theoretical insights are needed and it should not be ruled out yet.

Subject headings: globular clusters: general — globular clusters: individual (M5) — stars: evolution – stars: abundances

1. Introduction

By virtue of their large populations of coeval stars, the Galactic globular clusters present us with a unique laboratory for the study of the evolution of low mass stars. The combination of their extreme ages, compositions and dynamics also allows us a glimpse at the early history of the Milky Way and the processes operating during its formation. These aspects become even more significant in the context of the star-to-star light element inhomogeneities found among red giants in every cluster studied to date. The large differences in the surface abundances of C, N, O, and often Na, Mg, and Al have defied a comprehensive explanation in the three decades since their discovery.

Proposed origins of the inhomogeneities typically break down into two scenarios: 1) As C, N, O, Na, Mg, and Al are related to proton capture processes at CN and CNO-burning temperatures, material cycled through a region in the upper layers of the H-burning shell in evolving cluster giants may be brought to the surface with accompanying changes in composition. While standard models of low mass stars do not predict this “deep mixing”, several theoretical mechanisms have been proposed (e.g., the meridional mixing of Sweigart & Mengel 1979, and turbulent diffusion, Charbonnel 1994, 1995) with varying degrees of success. Moreover, there is ample observational evidence that deep mixing *does* take place during the red giant branch (RGB) ascent of metal-poor cluster stars (see the reviews of Kraft 1994 and Pinsonneault 1997 and references therein). 2) It has also become apparent that at least some component of these abundance variations must be in place before some cluster stars reach the giant branch. Spectroscopic observations of main sequence turn-off stars in 47 Tuc (Hesser 1978; Hesser & Bell 1980; Bell, Hesser, & Cannon 1983; Briley, Hesser, & Bell 1991; Briley *et al.* 1994, 1996; Cannon *et al.* 1998) and NGC 6752 (Suntzeff & Smith 1991, Gratton *et al.* 2000), as well as our own work in M71 (Cohen 1999, Briley & Cohen 2001, Ramírez & Cohen 2002) have shown variations in CN and CH-band and Na line strengths consistent with patterns found among the evolved giants of these clusters. The assumption that these low mass cluster stars are incapable of both deep dredge-up and significant CNO nucleosynthesis while on the main sequence leads to the possibility that the early cluster material was at least partially inhomogeneous in these elements or that some form of modification of these elements has taken place within the cluster. Suggested culprits include mass-loss from intermediate mass asymptotic giant branch stars and supernovae ejecta (see Cannon *et al.* 1998 for an excellent discussion of these possibilities).

Thus the observed light element inhomogeneities imply that there is some aspect of the structure of the evolving cluster giants which remains poorly understood (the deep mixing mechanism), that the early proto-clusters may have been far less homogeneous, that intermediate mass stars may have played a greater role in setting the composition of the present day low mass stars than previously thought, etc. Indeed, the evidence cited in the reviews above has led many investigators to suggest that a combination of processes is responsible, i.e., many clusters contain star-to-star inhomogeneities established early in their histories which have subsequently been further altered by deep mixing during the ascent of the RGB. This of course greatly exacerbates the difficulty of achieving an understanding of these issues, as a knowledge of the composition of the more easily observed bright red giants will not tell the whole story of their chemical history - one must also understand the makeup of the main sequence stars.

In the present paper, we continue our earlier work on M71 by exploring the CH and CN band strengths in a sample of low luminosity stars in the somewhat more metal poor globular cluster M5. We adopt current values from the on-line database of Harris (1996) for the apparent distance modulus of M5 at V of 14.31 mag with a reddening of $E(B-V) = 0.03$ mag. Recent CCD photometric studies of this cluster, focusing primarily on its age, are given by Johnson & Bolte (1998) and Stetson *et al.* (1999). Sandquist *et al.* (1996) discuss the predominantly blue horizontal branch of M5. We adopt the metallicity $[Fe/H] = -1.21$ dex found by Ivans *et al.* (2001) in a high dispersion abundance analysis of a large sample of stars on the upper giant branch of M5.

We describe the sample in §2 and 3. We outline our measurement of the molecular band indices and their interpretation in terms of the scatter in §4. With an assumption about the O abundance, these are converted into C and N abundances, from which we find a strong anti-correlation between C and N in §5. A discussion of our results together with a comparison with the trends seen among the red giants in M5 and in other globular clusters is given in §7.2 and 8. A brief summary concludes the paper.

2. Photometric Database

The photometry of M5 employed here was carried out as part of a larger program to provide homogeneous photometry for star clusters and nearby resolved galaxies (Stetson, Hesser & Smecker-Hane 1998, Stetson 2000). In the present instance, the photometry is based on data obtained during 18 observing runs between 1984 and 1998. Of these, some observing runs were carried out by PBS, data from other runs were donated by collaborators (M. Bolte, J. Hesser, R. McClure, N. Suntzeff), and data from still other runs were obtained through the services of the Isaac Newton Group Archive. Data origins include the 4m and 0.9m telescopes on Kitt Peak and Cerro Tololo, the Canada-France-Hawaii Telescope, the Isaac Newton Telescope, and the Jacobus Kapteyn Telescope.

⁷ In all, some 374 images of parts of M5 in filters corresponding to the *BVI* bandpasses were analyzed. Since different field sizes and different field centers were available from the various observing runs, no individual star actually appeared in more than 226 of those images.

Employing only data obtained under photometric conditions on nights when numerous observations of fundamental and secondary standards (see Stetson 2000) were also obtained, we defined a network of 649 local photometric standards in the M5 field. A star was considered a “local standard” in a given photometric bandpass only if it had been measured in that bandpass under photometric conditions on at least five occasions, if the standard error of the mean magnitude in that bandpass was less than 0.02 mag, *and* if the star showed no evidence for intrinsic variability greater than 0.05 mag, root-mean-square, in excess of random measuring errors when all bandpasses were considered together. Once this network of local standards had been created, it was possible to use them to calibrate the zero points of frames taken under non-photometric conditions (the color terms of the photometric transformations having been obtained through observations of fundamental standard fields), allowing us to include these latter frames in the overall photometric solution. Adding images taken under non-photometric conditions does nothing to improve the accuracy of our photometric transformations to the fundamental standard system in absolute terms; however, it does allow us to increase the precision of the photometry of individual stars relative to the mean system defined by our 649 local photometric standards.

In our experience, photometry from datasets such as those employed here typically display an external accuracy of roughly 0.02 mag per observation; this level of observation-to-observation scatter is probably dominated by temporal and spatial fluctuations in the instantaneous atmospheric extinction, and probably also by the difficulty of obtaining truly appropriate flat-field corrections in the presence of such effects as scattered light, ghosts, fringing and spectral mismatch between the flat-field illumination and the astronomical scene. In the present instance, our absolute photometry for the 649 local standards is based upon a median number of 10, 29, and 19 observations in the *B*, *V*, and *I* bandpasses. Taking 0.02 mag per observation as a typical external uncertainty, we therefore expect that our photometry is referred to the fundamental system (i.e., that of Landolt 1992) with an absolute accuracy of order 0.006, 0.004, and 0.005 mag, standard error of the mean, in *B*, *V*, and *I*. *Relative* magnitude and color differences among different stars in our sample can be smaller than this, depending upon their brightness and crowding and the number of observations that went into each determination.

The absolute astrometry of our catalog is based upon the United States Naval Observatory Guide Star Catalogue I (A V2.0; henceforth USNOGSC, Monet *et al.* 1998), access to which is obtained by PBS through the services of the Canadian Astronomy Data Centre. The authors of the USNOGSC claim a typical astrometric error of 0.25 arcsec, which they believe is dominated

⁷Although some Keck images are available, very short exposure times of only 1 or 2 seconds were used, and the photometric accuracy of the data is then compromised at the level of 2% due to issues involving the shutter open/close time and its uniformity over the field. In addition, the field of the available Keck images is small.

by systematic errors in the calibration procedure. When transforming relative (x, y) positions from large-format CCD images to absolute right ascensions and declinations from the USNOGSC for stars in common, we typically find root-mean-square differences of 0.3 to 0.4 arcsec in each coordinate. Some of this is clearly due to proper-motion displacements accumulated during the forty-plus years between the obtaining of the first Palomar Observatory Sky Survey and our CCD data. However, a significant part of the differences is also due to the lower angular resolution of the Schmidt plates as scanned by the Precision Measuring Machine (built and operated by the U. S. Naval Observatory Flagstaff): particularly in crowded fields such as the outskirts of globular clusters, a single entry in the USNOGSC is occasionally found to correspond to the photocenter of a close pair or a clump of several stars in the CCD imagery.

As a result of these non-Gaussian errors (i.e., proper motions and blending), we perform our astrometric transformations using an iterative procedure wherein 20-constant cubic polynomials are used to approximate the transformation of the (x, y) positions measured in our CCD images to standard coordinates obtained from a gnomonic projection of the right ascensions and declinations listed in the USNOGSC. After each iterative step, stars lying within a certain radial distance of their predicted positions are used to obtain an improved geometric transformation with individual weights gradually tapering from 1.0 for perfect positional agreement to 0.0 for stars lying exactly one critical radius from their predicted positions; stars lying farther than one critical radius from their predicted positions are ignored altogether. The critical radius distinguishing acceptable cross-identifications starts out fairly generous (~ 5 arcsec), but then this radius is gradually reduced until it is down to a value of one arcsecond; the iterative process then continues, maintaining this critical radius of one arcsecond, until a stable list of cross-identifications and transformation constants is achieved. As an indication of the percentage of entries in the USNOGSC whose positions we consider no longer strictly valid, due either to proper motions or to blending, we find that 4,709 USNOGSC entries lie within 5 arcsec of one of our CCD detections; 4,652 lie within 2 arcsec of a CCD detection; and 3,886 lie within 1 arcsec. When the sample is restricted to these 3,886 cross-identifications, the unweighted root-mean-square positional difference is approximately 0.34 arcsec in both x and y . Thus, what is essentially a $3\text{-}\sigma$ clip results in a rejection of some 17% of the “possible” cross-identifications that agree to within 5 arcsec.

Of these 3,886 acceptable cross-identifications, only a dozen or so lie within 200 arcsec of the cluster center; none at all lie within 160 arcsec. Therefore it is possible that interpolation of the astrometric transformations across this gap could be subject to small systematic errors, probably not as large as 0.1 arcsec. Throughout the region of our field that is well populated by USNOGSC stars (including essentially all of the stars in our present spectroscopic sample), we expect systematic errors of our right ascensions and declinations on the system of the USNOGSC to be of order $0.34 \text{ arcsec} / \sqrt{3886 - 20}$, or ~ 0.01 arcsec. We have no independent information on the accuracy with which the USNOGSC coordinate system is referred to an absolute inertial reference frame of right ascension and declination. Individual *random* errors in our coordinate measurements are probably not much better than 0.02 arcsec on a star-by-star basis, the errors becoming somewhat

worse than this for the fainter and more crowded stars in our photometric/astrometric sample.

Stars are identified in this paper by a name derived from their J2000 coordinates, so that star C12345_5432 has coordinates 15 12 34.5 +2 54 32.

3. Spectroscopic Observations

The initial sample of stars consisted of those from the photometric database located more than 150 arcsec from the center of M5 (to avoid crowding) with $16.9 < V < 17.35$ and with $0.86 < (V - I) < 0.96$, i.e. subgiants at the base of the RGB. (A preliminary version of the photometric catalog described in §2 was used for this purpose.) From this list, two slitmasks containing about 25 slitlets each were designed using JGC’s software. The center of the first field was roughly 3.2 arcmin E and 0.5 arcmin S of the center of M5, while the center of the second field was located roughly 2.5 arcmin W and 0.5 arcmin S of the cluster center.

These slitmasks were used with LRIS (Oke *et al.* 1995) at the Keck Observatory in May 2001; three 800 sec exposures were obtained with each slitmask. The exposures were dithered by moving the stars along the length of the slitlets by 2 arcsec between each exposure. Because of the crowded fields, there were often more than one suitably bright object in each slitlet. Hence subtraction of sequential exposures was not possible, and they were reduced individually using Figaro (Shortridge 1988) scripts, then the 1D spectra for each object were summed. The width of the slitlets was 0.7 arcsec, narrower than normal to enhance the spectral resolution. LRIS-B was used with a 600 line grism giving a dispersion of $1.0 \text{ \AA}/\text{pixel}$ (3.0 \AA resolution for a 0.7 arcsec wide slit). This gave good coverage of the region from 3600 to 4800 \AA , including the key CN band at 3885 \AA and the G band of CH at 4300 \AA . Technical problems related to the layout of the slitmasks led to some of the spectra not extending blue enough to reach the uv CN band. The red side of LRIS was configured to use a 1200 g/mm grating centered at $H\alpha$ with the intention of providing higher accuracy radial velocities. The dispersion is then $0.64 \text{ \AA}/\text{pixel}$ ($29 \text{ km s}^{-1}/\text{pixel}$) or $1.9 \text{ \AA}/\text{spectral resolution element}$. Unfortunately, the LRIS-R shutter was not functioning on the first night, and so only one of the two slitmasks used has matching $H\alpha$ spectroscopy.

In addition to the primary sample described above, since these fields are rather crowded, other stars sometimes serendipitously fell into the slitlets, and their spectra were also reduced. We refer to the latter as the secondary sample. As might be expected from the luminosity function, most of the secondary sample consists of stars at or just below the main sequence turnoff. Two stars in the secondary sample (C18386_0713 and C18465_0214) are early type stars. The former is almost certainly a BHB in M5, while the status of the latter is unclear; we subsequently ignore both of them.

3.1. Membership

Given the high galactic latitude of M5 ($b = 46.8^\circ$) and the proximity of our fields to the center of the cluster, we expect minimal field star contamination among the primary sample of stars. However, the secondary sample selection is based solely on spatial position and hence may contain a higher fraction of field stars. There are three indicators we use to establish membership. The first is deviation from the cluster sequences in a color-magnitude diagram. Stars which are off the M5 color locus in the (V, I) CMD by more than 0.1 mag were considered possible non-members. The second is the strength of the absorption features in the LRIS multi-slit spectra, ignoring the molecular bands. The metallicity of M5 is sufficiently low that near solar metallicity field stars of similar colors are easily distinguished from cluster members. We also examine the radial velocity by cross correlating the red spectra over the regime from 6400 to 6620 Å.

The radial velocity of M5 from the compilation of Pryor & Meylan (1993) is $+53.1 \text{ km s}^{-1}$, with $\sigma = 4.9 \text{ km s}^{-1}$. The histogram of heliocentric radial velocities we have measured for 37 stars is given in Figure 1. Only one star has a radial velocity inconsistent with membership. Rejecting this very discrepant object, with 36 remaining stars, we find a mean $v_r = +52.8 \text{ km s}^{-1}$, with $\sigma = 11.8 \text{ km s}^{-1}$. This value of σ corresponds, after removing the intrinsic stellar velocity dispersion, to an instrumental error of 0.4 pixels in the focal plane CCD detector of LRIS-R, which seems reasonable.

Table 1 gives a listing of those stars in our sample which are probably not members based on these three tests. The final column gives the distance in $(V - I)$ color at the fixed V mag of the star between the color of the star and that of the cluster locus. There are two definite non-members which appear to be more metal rich field stars. There are three stars which are off the cluster (V, I) color locus by slightly more than the adopted cutoff of 0.1 mag, but which we believe to be cluster members; all of them are crowded with a star of comparable brightness within 2 arcsec, and all are from the primary sample. There is also one faint star from the secondary sample which is either a blue straggler in M5 or an early type background object, and which we subsequently ignore.

Spectra taken with the blue-side of LRIS are available for all the stars, but at a lower dispersion. After excluding the probable non-members listed in Table 1, cross correlations over the range 3800 - 4400 Å show the same 1σ rms dispersion as does the red side, i.e. 0.4 pixels, here equivalent to 29 km s^{-1} . While the accuracy of these radial velocities, given the low spectral resolution, is not sufficient to confirm membership for any particular star, the small dispersion does demonstrate that almost all of the sample studied here must be members of M5.

3.2. The Sample of Probable Members of M5

There are 59 stars left in our M5 sample after the probable non-members and early type stars have been eliminated. In Figure 2 these are shown superimposed on the (V, I) CMD diagram, where a decreasing fraction of stars in the photometric database are plotted as V becomes fainter

to maintain clarity in the figure. All but one of these are at least 1.5 mag fainter in V than the HB in M5; there is no possible confusion with AGB stars at these low luminosities.

Figure 3 shows the region of the 4300 Å G band of CH in the spectra of two of the stars in the primary sample. These stars have essentially the same stellar parameters (T_{eff} and $\log(g)$) lying at about the same place in the cluster CMD, yet their G bands differ strongly. The CN band near 4200 Å is too weak to be used in these metal poor stars; the ultraviolet CN band near 3885 Å must be used instead. From this figure alone, we can anticipate one of the key results of our work, the large scatter in C abundance we will find among M5 members at the base of the RGB at $V \sim 17.2$ mag. We can also see that the CN bands are much weaker, and a careful measurement will be required, which is complicated by the difficulty of measuring anything resembling a continuum at or near 3885 Å.

Table 2 lists the photometry for the sample of 59 stars (plus one BHB star) which we believe are members of M5.

4. Measurement of CH and CN Indices

For each spectrum, S(3839) and I(CH) indices sensitive to absorption by the 3885 Å CN band and the 4300 Å CH band respectively (see Briley & Cohen 2001) were measured. These indices are listed in Table 3 and plotted in Figure 4. The error bars (drawn at 2σ) have been calculated strictly from Poisson statistics based on the signal present in the feature and continuum bandpasses.

It is extremely difficult to flux spectra taken through slitmasks because of the varying slit losses and the possibility of atmospheric dispersion affecting the spectra. The latter issue is of somewhat more concern than usual to us since we are working in the blue and UV with a narrow (0.7 arcsec wide) slit. Carrying out the observations with the length of the slit set to the parallactic angle, which is the usual method for eliminating atmospheric dispersion for single slit observations, cannot be used for multislit observations as the position angle is fixed by the design of the slitmask. It is for these reasons that no attempt was made to flux the spectra.

The reduction process for the G band index of CH, whose feature bandpass is 4285 - 4315 Å (adjusted by 0.76 Å for the average radial velocities of the present stars), is independent of this suite of issues as a continuum can be established both on the blue and on the red side of the feature. However, it is extremely difficult to establish a continuum on the blue side of the 3885 Å CN band, and hence we are forced to rely on a single sided index, with a continuum bandpass determined only redward of the feature of interest.

The instrumental signature present in the raw S(3839) indices, whose feature bandpass is 3846 - 3883 Å (shifted by 0.68 Å), must be removed prior to a comparison with those predicted by models. This was carried out following Briley & Cohen (2001) by fitting the continua of the observed spectra with cubic splines within IRAF’s “splot” facility over the range 3600 - 5200 Å.

The I(CH) indices determined from these continuum fits (with no CH absorption included) were effectively zero (-0.008 ± 0.007) as is expected from a two-sided index.

For S(3839), indices were computed from these continua fits and the average (0.156 ± 0.019) used as a zero-point offset (as follows from the logarithmic nature of S(3839)) in our comparisons. Stars with spectral coverage ending redward of 3820 \AA were not included. The process used to determine the zero point offset for the uvCN indices thus assumes that the transmission $T(\lambda)$ of the atmosphere, telescope and instrument (including slit losses) normalized to the transmission at some fiducial wavelength, e.g. 4000 \AA , is a function of wavelength which does not change among the spectra of the M5 stars over the relevant wavelength range, i.e. that of the two bands used to define S(3839), from 3840 to 4000 \AA ; this is a less stringent requirement than would be needed to flux the spectra.

Slit alignment errors which vary from star to star (possible with the narrow 0.7 arcsec wide slits used here) combined with atmospheric dispersion are the most likely way to introduce a variation in the normalized $T(\lambda)$ from star to star, which would in turn introduce a dispersion in S(3839) through variation of the zero point from that adopted above. The two slitmasks used for our M71 sample were observed at mean airmasses of 1.08 and 1.25 respectively. This should be adequate to avoid serious problems with atmospheric dispersion. Cohen & Cromer (1988) discuss this issue in more detail.

We have tested the correlation between fit uv continuum slope and various parameters, including RA, Dec, luminosity and S(3839). The correlations range from not statistically significant to marginally significant, with the correlation between uv continuum slope and S(3839) being the most significant (correlation coefficient of 0.48) and that with luminosity being the least significant (correlation coefficient 0.09).

The small corrections derived from these correlations have a maximum value of about 0.015 and a minimum value of 0.000 , which is less than 5% of the total range and smaller than the quoted uncertainties. Given that the S(3839) variations among the stars in our sample of subgiants in M5 cover a range of roughly 0.3 in S(3839), these small corrections, if implemented, would have little affect on our resulting C and N abundances, and we have elected not to include them.

As can be seen in Figure 4, a substantial star-to-star variation is seen among I(CH) indices for the stars in our M5 sample, even if one considers only subgiant branch (SGB) stars in similar evolutionary states. To aid in interpretation, the stars in Figure 4 have been arbitrarily divided into CH-weak (open symbols) and strong groups (filled symbols).

Six of the stars with the most extreme CH or CN indices are denoted as anomalous. Of these, five have radial velocities, all consistent with membership in M5. Four of these stars are in the sample at the base of the RGB and show very strong I(CH) with very weak CN. C18225_0537 has $V = 18.06$ and shows an enormous I(CH) with a strong S(3839) as well. C18206_0533 ($V = 18.42$) shows modest I(CH) but very strong uv CN. For the brighter of these stars, the anomaly noted in the final summed spectra is clearly present on each individual spectrum of the object, and hence it

is highly unlikely that these anomalies are due to CCD defects or other such problems. We plan to check the membership of each of these stars with higher dispersion spectra as soon as possible, but at the present time, we believe that most, if not all, of these anomalous stars are in fact members of M5.

We proceed by restricting our attention to the subgiants at the base of the RGB in M5, specifically to those with $16.5 < V < 17.5$ mag. Figure 5 displays I(CH) versus S(3839) for this group of 43 stars. Again the very large range in each index within this small range in evolutionary state, hence small range in T_{eff} and $\log(g)$, is apparent. Also apparent is a strong anti-correlation between the strength of the CH band and that of the CN feature. The correlation is not perfect, and tends to turn over among the stars with the weakest I(CH). The bimodal distribution of CN band strengths found among the most luminous M5 giants by Smith & Norris (1983) is also not apparent in the present sample. This may be the result of the higher temperatures (and correspondingly weaker CN bands) of our stars, combined with a finite observational error tending to blur out the bimodality.

The large range in C abundances which we suspect to be present in the M5 subgiant sample creates an unusual situation with regard to the expected strength of the CN features. Normally, since there is more carbon than nitrogen, the N abundance controls the amount of CN. However, if C is highly depleted, there can be fewer carbon atoms per unit volume than nitrogen atoms, and C will control the formation of CN, as suggested by Langer (1985). Within the small range of T_{eff} covered by the M5 subgiant sample, we might expect the observed relationship between the molecular band indices of CH and of CN to be non-monotonic, as is in fact shown in Figure 5. In particular, in this figure, the stars with the weakest CH do not have the strongest CN indices.

4.1. The Main Sequence Turn Off Stars

There are twelve stars in our sample with $V > 18.2$ which are believed to be members of M5 at or slightly fainter than the main sequence turnoff (MSTO). Their molecular bands are, as expected, much weaker due to their higher T_{eff} . However, it does appear that variations in I(CH) are still present, although not as large in extent as are seen among the subgiants. Figure 6 presents the region of the G band of CH in four of the main sequence stars in M5 in order of increasing V mag. They span a total range of 1.4 mag in V from the top of the main sequence downward in luminosity and cooler in T_{eff} . The spectra have been slightly smoothed using a Gaussian with FWHM of 5 pixels, then a continuum was fit from 3900 to 4500 Å, and the spectra were normalized. The signal-to-noise ratio of the spectra decreases as the magnitude increases. The CH band is marginally stronger in the first star than in the second, and strongest in the coolest star, much stronger than in a main sequence star only 0.2 mag brighter. The strongest atomic features, particularly the Ca I lines at 4226 Å and the Fe I lines at 4046 and 4384 Å, are also becoming stronger as T_{eff} decreases. Higher precision data and a larger sample of main sequence turnoff stars will be required to determine in a definitive way the trends among CH and CN.

5. Comparisons with Synthetic Spectra

Clearly the pattern of abundances underlying the CH and CN band indices of Figure 4 cannot be interpreted on the basis of band strengths alone - we must turn to models. The technique employed is similar to that of Briley & Cohen (2001), where the region of the CMD of interest is fit by a series of models whose parameters are taken from the Bergbusch & Vandenberg (1992) O-enhanced isochrones. For M5, the 16 Gyr isochrone with $[\text{Fe}/\text{H}] = -1.26$ was used to select a set of representative model points which are listed in Table 4. Model stellar atmospheres were then generated using the Marcs model atmosphere program (Gustafsson *et al.* 1975) at the T_{eff} , $\log(g)$ of these points. From each model, synthetic spectra were calculated using the SSG program (Bell & Gustafsson 1978; Gustafsson & Bell 1979; Bell & Gustafsson 1989; Bell, Paltoglou, & Tripicco 1994) and the line list of Tripicco & Bell (1995). Each synthetic spectrum was initially computed from 3,000 to 12,000 Å in 0.1 Å intervals and convolved with V and I filter curves as described in Gustafsson & Bell (1979) and Bell & Gustafsson (1989) to yield colors appropriate to each model.

Figure 7 shows these model points superposed on the M5 V, I CMD. We assume stellar masses as given by the isochrone, a microturbulent velocity of 2 km/s, and the cluster parameters given in §1. As is apparent from the Figure, the isochrone closely follows the M5 CMD. We have compared T_{eff} derived from the isochrone itself, which values we subsequently adopt, with T_{eff} derived from the observed $V - I$ colors of each of the subgiants individually. We use the grid of predicted colors from Houdashelt, Bell & Sweigart (2000) for this purpose, together with the $\log(g)$ from the isochrone. (The dependence on $\log(g)$ is relatively small.) The mean difference is $\sim +70\text{K}$, with a large σ of 90 K. While some part of this mean difference might be photometric errors, if interpreted as an error in matching the color of the isochrone at a fixed V with the locus of the M5 stars, this corresponds to a systematic difference in $V - I$ of about 0.03 mag. A hint of this is seen in Figure 7, where the cluster locus does appear slightly redder than the adopted model points near $V \sim 17.5$. Ignoring these small differences, we therefore believe that assigning $T_{eff}, \log(g)$ utilizing the V mag plus the isochrone is a reasonable way to represent the mean properties of the M5 subgiant sample as a function of luminosity.

Using these models we have further calculated a series of synthetic spectra at higher resolution (0.05 Å intervals) from 3500 to 5500 Å with a variety of C, N, and O abundances. These spectra were then smoothed to the resolution of the observed spectra and the corresponding I(CH) and S(3839) indices measured. Zero point shifts were also measured from the synthetic spectra by loading them into IRAF and performing the continuum fits discussed above for the observed spectra. The resulting offset for S(3839) was 0.046 ± 0.010 and 0.003 ± 0.001 for I(CH).

The values of I(CH) from five sets of models with $[\text{C}/\text{Fe}]$ from -0.35 to -1.10 , $[\text{O}/\text{Fe}] = +0.25$, and $\text{C}^{12}/\text{C}^{13} = 10$ are plotted with the observed indices in Figure 8. The spread in $[\text{C}/\text{Fe}]$ among the M5 SGB stars appears well represented by this range, which is very similar to that reported among a sample of more luminous M5 SGB stars by Briley *et al.* (1992) (although a lower value of $[\text{Fe}/\text{H}] = -1.40$ was chosen in their study). We note the very low C abundances implied by the

weakest I(CH) indices among the SGB sample, which are consistent with the low C abundances observed among the brightest M5 giants (Smith *et al.* 1997). However, in the albeit small Smith *et al.* sample of five giants, no analog to the CH-strong stars (at least in terms of [C/Fe]) were observed.

The large range in C abundances indicated in Figure 8 leads to a difficulty in assessing N abundances via CN band strengths, as discussed in §4. Among the CH-strong SGB stars (see the left panel of Figure 8) there is a small (≈ 0.1 dex) spread in [C/Fe], with N being the minority species controlling the formation of CN. Thus, the CN band strengths of these stars can be assumed to roughly represent the [N/Fe] abundances. This is demonstrated in Figure 9 (left), where the S(3839) indices are compared to those from two series of synthetic spectra, the first with [C/Fe] = -0.35 , [N/Fe] = $+0.10$ and the second with [C/Fe] = -0.45 , [N/Fe] = $+1.00$ (with [O/Fe] = $+0.25$ and $C^{12}/C^{13}=10$ for both, as in Figure 8). Clearly the star-to-star spread in N abundances of the CH-strong SGB stars approaches a factor of 10.

For the CH-weak stars, the situation is more complex - the lower C abundances can regulate CN formation. Thus, as suggested by the discussion of §4, the large spread in [C/Fe] among the CH-weak stars essentially destroys any relation between S(3839) and N abundance. This is illustrated in Figure 9 (right) where S(3839) indices from model spectra with three different combinations of [C/Fe] and [N/Fe] are plotted. While [C/Fe] = -0.65 , [N/Fe] = $+1.20$ results in the stronger of the CN bands, the models with [C/Fe] = -0.55 , [N/Fe] = $+0.75$ have CN band strengths essentially indistinguishable from [C/Fe] = -1.10 , [N/Fe] = $+1.30$. Indeed, for the most C-poor of the current SGB stars, significant enhancements of N are required to reproduce the observed S(3839) indices.

We defer an attempt to deduce C and N abundances among the M5 main sequence turn off stars until a larger sample of spectra of such stars with higher signal-to-noise ratio than the present set of spectra becomes available.

6. Inferred C and N Abundances Among the Subgiants

To disentangle the underlying C and N abundances from the CH and CN band strengths, we have simultaneously fit the [C/Fe] and [N/Fe] abundances corresponding to the observed I(CH) and S(3839) indices of the SGB stars. The temperatures and gravities used for the models were chosen based on the V magnitudes of the observed stars in the present photometry as fit to the isochrone in Figure 2 using cubic splines. The validity of this procedure was established in §5. The abundances of C and N were then varied until the model I(CH) and S(3839) indices matched the observed values as closely as possible, including the derived zero points. The mean rms error in the fits to the observed indices was 0.005. For all stars, a value of [O/Fe] = $+0.25$, $C^{12}/C^{13}= 10$, and a microturbulent velocity of 2 km/s was assumed (the sensitivity to these assumptions will be explored below). The resulting C and N abundances for the M5 SGB stars are listed in Table 3 and plotted in Figure 10.

Immediately apparent in Figure 10 is a dramatic anti-correlation between the C and N abundances of the M5 SGB stars. Also plotted are the $[C/Fe]$ and $[N/Fe]$ abundances of a sample of more luminous M5 SGB stars reported in Briley *et al.* (1992) (note we have plotted the abundances from their $[Fe/H] = -1.25$ models), which compare very well with the present results. The error bars were determined by repeating the fitting process while including shifts in the observed indices of twice the average error among the SGB indices as derived from Poisson statistics (0.005 in $I(CH)$ and 0.02 in $S(3839)$). The shifts were included in opposing directions (e.g., +0.005 in $I(CH)$ and -0.02 in $S(3839)$, followed by -0.005 in $I(CH)$ and +0.02 in $S(3839)$) and reflect likely errors in the abundances due to noise in the spectra.

Of much greater concern are the systematic errors, as they have the potential to exaggerate any C versus N anticorrelation (i.e., stars with overly low C abundances will naturally require greater abundances of N to match the observed CN band strengths). To assess the role of many of our assumptions in shaping Figure 10, we have chosen three representative SGB stars and again repeated the fitting of the CN and CH band strengths with different values of $[Fe/H]$, $[O/Fe]$, C^{12}/C^{13} , etc. These results are presented in Table 5, where it may be seen that the sensitivity of the derived C and N abundances to the choice of model parameters is remarkably small (well under 0.2 dex for reasonably chosen values), as would be expected from these weak molecular features. We have also plotted the SGB C and N abundances as both functions of V and $V - I$ colors in Figure 11 to evaluate possible systematic effects with luminosity (albeit over a small range) and temperature; none appear to be present.

Evaluating the absolute abundance scale is more difficult as external comparisons are limited. For the main sequence stars in 47 Tuc, we can compare the results of Briley *et al.* (1991, 1994), carried out in a manner fairly similar to the present work, with the independent analysis of a different sample of stars by Cannon *et al.* (1998). This suggests we may be systematically underestimating the absolute C abundance by about 0.15 dex, and overestimating the N abundance by about 0.2 dex. However, such a shift cannot account for the large range in C and N abundances apparent in Figure 10. We therefore conclude that the C versus N anti-correlation among the SGB stars in Figure 10 is indeed real.

7. Review of Previous Studies of C and N in Globular Clusters

7.1. The Case of M5

There have been several previous studies of the C and N abundances in M5. Smith & Norris (1983) measured CH and CN indices for a sample of 29 stars near the RGB tip. They found a bimodal distribution of CN absorption. Langer *et al.* (1985) reobserved six stars selected from this sample, three CN-strong and three CN-weak, and calculated the change in mean C and N abundance between the two groups. Briley *et al.* (1992) observed 14 subgiants with $16.2 < V < 16.5$, analyzed in a manner similar to the present paper, to find large stochastic variations from star-to-star of

a magnitude similar to those found here for still fainter subgiants, and with a clear detection of bimodality for the S(3839) indices of these subgiants.

A question of considerable import for understanding the behavior of C and N in M5 is whether or not there is any change in the mean C abundance as one moves from the RGB tip down to the base of the subgiant branch. Any effect dependent on evolutionary state is an argument favoring internal mixing rather than an external (primordial or pollution) origin for this phenomenon. While this issue is complicated by the need to convert between three different definitions for the strength of absorption at the G band of CH, the best that can be said at the present time is that any difference in the mean $[C/H]$ between the tip and the base of the RGB in M5 must be less than 0.3 dex. We seem to be in the peculiar position of having a better sample of stars with published C and N abundances between $16.0 < V < 17.5$ than exists at the RGB tip. We have already initiated an effort to remedy this and to refine this crucial number.

7.2. Other Globular Clusters

Cohen (1999) has shown that the C/N anti-correlation seen among bright RGB stars in M71 extends to the stars at the main sequence turnoff and even fainter in M71. At the level of the main sequence, the distribution of both the CH and CN indices appears to be bimodal. Briley & Cohen (2001) have used model atmospheres combined with synthetic spectra in an approach similar to that of the present paper to show that the C and N abundance range seen at the level of the main sequence is comparable to that seen among the bright red giants of M71 by many previous studies, the most recent of which is Briley, Smith & Claver (2001). To reproduce the M71 CH and CN bands requires a range in C of a factor of 2 starting from $[C/Fe] = 0.0$ and a range in N of a factor of 10, starting from an initial N enhancement of a factor of 2.5 ($[N/Fe] = +0.4$ dex, together with a decrease in O from $[O/Fe] = +0.4$ to $+0.1$). These numbers are very similar to what is required to explain the M5 subgiants, with the exception of $[C/Fe]$, which exhibits a larger variation among the M5 subgiants (a factor of 6 versus 2).

Norris, Freeman & DaCosta (1984) studied the CH and CN indices among a sample of 112 bright RGB stars in 47 Tuc (a high metallicity cluster, with $[Fe/H]$ similar to that of M71), while Cannon *et al.* (1998) observed a sample of comparable size from the base of the RGB to the upper main sequence. Large stochastic star-to-star variations with similar anti-correlations between C and N abundances and with a bimodal behavior of CN were found at all luminosities examined. The range of mean abundances between the CN-strong and CN-weak groups appeared unchanged from the lower RGB to the main sequence, with the CN-strong group having $\langle [C/H] \rangle = -0.15$, $\langle [N/H] \rangle = +1.05$ dex, as compared to $\langle [C/H] \rangle = +0.06$, $\langle [N/H] \rangle = +0.20$ dex for the CN-weak stars. The N range is comparable to that found here for M5, but again, as with M71, the C range is a little smaller in 47 Tuc. Similar to the situation in M5, large samples exist both at the tip of the RGB and at the main sequence in 47 Tuc, but they are not well tied together, and it is not possible from the published papers themselves to establish the magnitude of any systematic change

in the mean $\langle [C/H] \rangle$ with luminosity, beyond a statement that it cannot be large.

Determinations of the C^{12}/C^{13} ratio have been made for the brightest RGB stars in 47 Tuc by Brown, Wallerstein & Oke (1990) and Bell, Briley, & Smith (1990), as well as in M71 by Briley *et al.* (1997). They obtain $C^{12}/C^{13} \sim 4 - 8$, correlated with CN-band strength, implying that the surface C-poor, N-rich envelope material has been exposed to proton capture.

The seminal survey of C and N in the intermediate metallicity clusters M3 and M13 (two clusters of slightly lower metallicity than M5) by Suntzeff (1981) established the existence of a bimodal distribution of CN band strength, at least for $M_V \lesssim -0.4$, with stochastic variations in C and N abundance from star to star in each cluster. Smith *et al.* (1996) combine their C and N abundances for a sample of stars near the tip of the RGB in each cluster with published O abundances to show that the total of C+N+O is constant for these luminous giants.

The only other cluster with similar data available for its MSTO stars is NGC 6752, a cluster of similar metallicity to M3 and M13. Suntzeff & Smith (1991) observed both CH and CN variations among its MSTO stars. Gratton *et al.* (2001) report an anticorrelation between O and Na, as well as between Mg, Al and C and N, similar to the relations found among the luminous giants. Suntzeff & Smith (1991) also found low (3 - 10) C^{12}/C^{13} ratios, which they attributed to some mixing taking place but with primordial variations already in place.

M92 was studied in detail by Carbon *et al.* (1982), who used the NH band at 3360 Å, as the CN bands become too weak at such low metallicities. They studied 45 giants and subgiants with $M_V < +2$ and found strong stochastic star-to-star variations over their full luminosity range of about a factor of 3 in C and a factor of 10 in N. However, C and N are not in general anti-correlated. The data for fainter stars is limited at present (at least by the standards of the large samples we have achieved for M71 and for M5). However, it is clear that in addition to the variations, there is an easily detectable systematic decrease in the mean C abundance by about a factor of 10 from the base of the RGB to the top of the RGB (Langer *et al.* 1986, Bellman *et al.* 2001). They argue that this is the key fact in establishing that internal mixing is the dominant effect controlling the C and N abundances in M92.

M15, with metallicity similar to M92, was studied by Trefzger *et al.* (1983). In a sample of 33 bright giants reaching to $M_V = +1.2$, they found strong stochastic star-to-star variations, and found that the mean $\langle C/C_0 \rangle$ declines with advancing evolutionary state, but the mean N abundance does not change. Furthermore, they found that N/N_0 was so large for about 1/3 of the sample that it could not be explained even by converting all C into N.

CH in the upper RGB stars in NGC 6397, another metal poor cluster, was explored by Bell, Dickens & Gustafsson (1979).

8. Discussion

The primary facts that we have established for M5 are that there are strong stochastic variations from star-to-star of both C and N, with C and N anti-correlated, similar to those seen in M71. These variations are definitely present among the subgiants at the base of the RGB to $M_V \sim +3$ and appear to extend to the main sequence stars as well. A question of considerable import for understanding the behavior of C and N in M5 is whether or not there is any change in the mean C abundance as one moves from the RGB tip down to the base of the subgiant branch such as is clearly seen in M15 and M92. As discussed in §7.2 above, the best that can be said at the present time is that, unlike the case of M92 or M15, any systematic decline in the C abundance with evolutionary state as one moves up the RGB appears to be small, < 0.3 dex.

8.1. Implications for Stellar Evolution

A classical review of post-main sequence stellar evolution can be found in Iben & Renzini (1983). Their description of the consequences of the first dredge up phase, the only dredge up phase to occur prior to the He flash, indicates that a doubling of the surface N^{14} and a 30% reduction in the surface C^{12} can be expected, together with a drop in the ratio of C^{12}/C^{13} from the solar value of 89 to ~ 20 , as well as a drop in surface Li and B by several orders of magnitude. Observations of field stars over a wide range of luminosities conform fairly well to this picture, see e.g. Shetrone *et al.* (1993), Gratton *et al.* (2001), although additional mixing of Li and lower than predicted ratios of C^{12}/C^{13} seem to occur even among field stars (do Nascimento *et al.* 2000).

To match the observations of variations in abundances among globular cluster red giants which far exceed those described above, additional physics must be introduced into calculations of dredge up in old metal poor stars. Relevant phenomena include meridional mixing as described by Sweigart & Mengel (1979) as well as turbulent diffusion (see Charbonnel 1994, 1995) and the insights of Denissenkov & Denissenkova (1990) concerning the importance of the $^{22}\text{Ne}(p, \gamma)^{23}\text{Na}$ reaction as a way to produce p-burning nuclei.

The clear prediction of the most current calculations of this type by Denissenkov & Weiss (1996), Cavallo, Sweigart & Bell (1998) and Weiss, Denissenkov & Charbonnel (2000) is that the earliest that deep mixing can begin is at the location of the bump in the luminosity function of the RGB which occurs when the H-burning shell crosses a sharp molecular weight discontinuity. Zoccali *et al.* (1999) have shown that the luminosity of the RGB bump as a function of metallicity as determined from observation agrees well with that predicted by the theory of stellar evolution. Bono *et al.* (2001) further suggest that the agreement between the predicted luminosity function and actual star counts along the RGB in the vicinity of the bump in a suite of globular clusters is so good that mixing cannot have occurred any earlier, otherwise the evolutionary lifetimes, and hence the observed luminosity function, of such stars would have been affected by the mixing of He.

Zoccali *et al.* (1999) give the expected location of the RGB bump in M5 to be 0.3 mag brighter than the HB, i.e. at $V \sim 14.8$ or $M_V \sim +0.5$. Yet we see strong star-to-star variations in C and N abundances as well as a strong anti-correlation between them within a large group of cluster members at $V \sim 17.1$ ($M_V \sim +2.8$), more than 2.3 mags fainter at the base of the RGB. We see hints of such variation continuing on the upper main sequence at $M_V \sim +3.7$.

The range of luminosity over which these C and N variations are seen is becoming more and more of a problem for any scenario which invokes dredge up and mixing. Unless we have missed some important aspect of stellar evolution with impact on mixing and dredge up, we must declare the mixing scenario a failure for the specific case of M5 from our present work and M71 from our previous work (and several other globular clusters as well from the work of others). Even the theoreticians in the forefront of this field are beginning to admit that deep mixing alone is not sufficient (Denissenkov & Weiss 2001, Ventura *et al.* 2001). Unless and until some major new concept relevant to this issue appears, we must now regard the fundamental origin of the star-to-star variations we see in M5 as arising outside the stars whose spectra we have studied here.

The strong anti-correlation between C and N, however, does suggest that CN-cycle material must be involved, and that this material has somehow reached the surface of these subgiant stars in M5. Since we know it cannot come from inside these stars, it must come from some external source. As reviewed by Lattanzio, Charbonnel & Forestini (1999), CN and ON cycling is known to occur in AGB stars, and AGB stars are also known to have sufficient dredge up to bring such material to their surfaces. We might speculate that the site of the proton exposure could be a previous generation of high mass stars, which then suffered extensive mass loss (either in or outside of binary systems) and polluted the generation of lower-mass stars we currently observe, while the higher mass stars are now defunct.

8.2. ON Burning

Let us adopt as a working hypothesis that the C and N abundance variations we are seeing in the present subgiants are the result of the incorporation of material exposed to the CN-cycle (i.e., proton capture reactions) in a now evolved population of more massive ($2 - 5M_{\odot}$) AGB stars, as was originally suggested in D’Antona, Chieffi & Gratton (1983). Indeed, recent models of metal-poor AGB stars by Ventura *et al.* (2001) suggest temperatures at the bases of the convective envelopes of such stars are capable of these reactions. The new generation of precision abundance analyses of globular cluster stars over a wide range of luminosity such as that of Ramírez & Cohen (2002) for M71 demonstrate that the abundances of the α -capture and s-process elements are constant, and so we further assume that the early cluster environment of M5 was not significantly polluted by the ejecta of even more massive stars.

We now investigate whether this hypothesis is consistent with the C and N abundances we have derived for the main subgiant sample of M5. Figure 12 shows the sum of the C and N abundance

as a function of the C abundance of the sample of M5 subgiants. The solid dot shows the predicted location assuming the initial C and N abundances (C_0 , N_0) are the Solar values reduced by the metallicity of M5 ($[\text{Fe}/\text{H}] = -1.2$ dex). Thus this is the initial location for no burning and for a Solar C/N ratio. If the present stars incorporated material in which just C was burned into N, then the locus of the observed points representing the M5 subgiant sample should consist of a single horizontal line, with the initial point, the presence of no CN-cycle exposed material, at the right end of the line (the maximum C abundance) and the left end of the line corresponding to a substantial fraction of the star’s mass (i.e. the atmosphere plus surface convection zone) including C-poor, N-rich AGB stellar ejecta. Furthermore, if the initial C/N ratio of the cluster is not Solar, then the locus should still be a horizontal line, but located at a different vertical height in this figure.

The maximum possible N enhancement for a cluster SGB star with these assumptions occurs if the star formed entirely from AGB ejecta in which all C has been converted into N. For initial values (C_0 , N_0) (not expressed as logarithms), this maximum N enhancement would be $(C_0 + N_0)/N_0$. If the initial value was the Solar ratio, $C_0/N_0 \sim 3.2$, the resulting maximum N enhancement is a factor of ~ 4.2 , while for an initial C_0/N_0 of 10, the maximum N enhancement is a factor of 11.

Now we examine the behavior of the C and N abundances among the M5 subgiant sample as inferred from our observations. It is clear that the assumption that the only thing happening is inclusion of material in which C was burned into N must be incorrect. The sum of C+N seems to systematically increase by a factor of ~ 5 between the most C rich star and most C deficient star. The discussion of the errors, both internal and systematic, in §6 suggest maximum systematic errors of -0.2 dex for $\log(\text{C}/\text{H})$ and $+0.2$ for $\log(\text{N}/\text{H})$. This is completely insufficient to explain such a large trend as errors.

We thus have a serious discrepancy. The sum of C+N was *not* constant as C was burned in the AGB sites. Furthermore the observed range in N abundances is very large. The most obvious way to reproduce this is to include O burning as well as C burning. If we adopt Solar ratios as our initial values, then a substantial amount of O burning is required.

Figure 12 suggests that the initial ratio of C/N is not quite Solar, although not too far off. Adopting the Solar value as the initial C/N ratio, we calculate the minimum amount of O which must be burned at the base of the AGB envelopes to reproduce the locus observed in the figure (under the arguable assumption of the most extreme of our stars having formed largely from such material - this will, however, provide us with at least an estimate of the minimum burning required). We need to produce a N enhancement of a factor of 10. The Solar ratio is $\text{C}/\text{N}/\text{O} = 3.2/1/7.6$, so if all the C and 50% of the O were converted, we have an enhancement of N of a factor of 8 available to the present stars. Oxygen is typically found to be overabundant with respect to Fe in old metal-poor systems (see Meléndez, Barbuy & Spite 2001, Gratton *et al.* 2001, Ramírez & Cohen 2002, and references therein); we assume $[\text{O}/\text{Fe}] \sim +0.3$ dex, a typical value. Then the initial C/N/O ratios will be $3.2/1/15.2$. Note that the same amount of O has to be burned to

produce the observed distribution of C and N abundances, but in this case it is a considerably smaller fraction of the initial O.

Returning to the AGB models of Ventura *et al.* (2001), the requirement for substantial O burning that emerges from our analysis of the CH and CN bands in the M5 subgiants may not be an unreasonable constraint - for metal-poor AGB stars they find temperatures sufficient for CNO-processing at the bases of AGB stars in a wide mass range. Following their $Z=0.001$ ($[\text{Fe}/\text{H}] = -1.3$) models we find surface O abundances dropping by a factor of 2 to 20 in masses from 4.5 to $2M_{\odot}$. We also note that under the assumption of little change in $[\text{C}/\text{Fe}]$ (less than 0.3 dex as discussed above) taking place during the RGB ascent of the present low mass M5 stars, one should also expect little change in $[\text{O}/\text{Fe}]$ as well, and that the O abundances of the present bright giants reflect their “primordial” values. The observed $[\text{O}/\text{Fe}]$ abundances of the bright M5 giants by Sneden *et al.* (1992) are not inconsistent with this idea. Their “O-rich” stars average around $[\text{O}/\text{Fe}] = +0.3$ while their most “O-poor” stars are depleted by a factor of 3.5. If this is the result of ON-cycle exposure, more than enough N can be produced to explain the present results.

This simple test is of course leaves significant questions unanswered. Problems include whether there were a sufficient number of AGB stars present to return the required quantity of material and the efficiency of any mechanism to incorporate it in the present stars. This is a non-trivial issue if the most C/O-poor, N-rich SGB stars formed with a preponderance of AGB ejecta - to reduce the C abundance by a factor of 6 by adding C-poor ejecta would require some 83% of the present star’s mass to be made of this material. Note, as has been pointed out by several authors, these abundance inhomogeneities cannot simply be surface contaminations as they would be diluted by the increasing depth of the convective envelope during RGB ascent. Also, the range of C abundances among the M5 SGB stars appears much larger than that of any cluster studied to date. While this can perhaps be explained with regard to the more metal-rich clusters, whose polluting AGB stars should have undergone less ON-cycling, other even more metal-poor clusters than M5 appear to have smaller star-to-star C variations among their less evolved stars. This can be seen in the $[\text{C}/\text{Fe}]$ versus luminosity diagrams of Carbon *et al.* (1982) and Bellman *et al.* (2001) for M92, where the range in $[\text{C}/\text{Fe}]$ among the least luminous stars is relatively small (certainly not the factor of 6 seen here in M5). But this may be perhaps explained by varying the efficiency for incorporating AGB ejecta into subsequent generations of stars among the proto-globular clusters.

Following Ventura *et al.* (2001), we predict substantial O variations, anti-correlated with Na and Al, to be present among the M5 subgiants and fainter stars. If the source of the proton exposed materials is indeed moderate mass AGB stars, these inhomogeneities should also correlate with Li abundances among the less evolved stars. We expect the verification or lack thereof of these predictions to be available shortly.

Another important point is that Figure 12 shows no evidence for any bimodality in the distribution of the C and N abundances for the small section of the subgiant branch in M5 covered by our sample. The distribution along the locus of abundance appears to first order to be uniform. There

is no preponderance for stars populating the extremes of high C or low C. An artificial suggestion of bimodality, or more correctly a tendency towards high CN strengths, could be produced by the distribution of C and N abundances shown in Figure 10 or by saturation effects in the molecular bands themselves, which would only become apparent in cooler stars with stronger molecular bands.

We also recall the anomalous stars in our sample, most of which are believed to be members of M5. Two of these in particular have enormously strong CH bands; we can offer no explanation for these stars at present.

8.3. Additional Implications for Stellar Evolution

Figure 12 was used above to demonstrate that ON burning is required by considering the required N enhancement factor. This figure also displays a correlation between the sum of C and N number densities with the C abundance, i.e. the C abundance is correlated with the C/N ratio among the M5 subgiant stars. Here we explore the consequences of the existence of this correlation for the origin of the C and N variations themselves. Any external mechanism for producing these variations will involve an efficiency factor for the incorporation of material. We expect this factor to depend on the mass of the star itself, how much additional mass is incorporated (ΔM), and the initial C and N abundances in the star itself and within ΔM . Since these properties of ΔM might be expected to fluctuate wildly, this process therefore should show a lot of stochastic random variability.

It is easy to imagine that various parcels of ΔM have a wide range in C/N ratios due to the varying amount of nuclear processing that each might have experienced, and thus the strong stochastic star-to-star variations in C and N as well as their overall anti-correlation that we observe among the M5 subgiants can be reproduced. However, the correlation above requires a correlation between the mass of the parcel accreted, ΔM , and the C/N ratio of the material within this mass, and that seems to be rather artificial given the random nature of the process. We thus conclude that is difficult to reproduce the correlation described above with such an external mechanism involving accretion of “polluted” material from AGB stars. Unless we have made gross errors in the C and N abundances in our M5 subgiant sample far beyond what we believe might have occurred, the existence of this correlation suggests that we should not totally rule out internal mechanisms as yet.

9. Summary

We have presented photometry and spectroscopy for a large sample of M5 subgiants and several main sequence turn off stars. An analysis of the SGB spectra reveals significant and anti-correlated star-to-star variations in C and N abundances, as would be expected from the presence of proton-capture exposed material in our sample stars. Similar variations in CH also appear to be present

in the main sequence turn off spectra, but the signal in the current sample is too low for a detailed analysis. The evolutionary states of these stars are such that the currently proposed mechanisms for *in situ* modifications of C, N, O, etc. have yet to take place. On this basis, we infer that the source of proton exposure lies not within the present stars, but more likely in a population of more massive ($2 - 5M_{\odot}$) stars which have “polluted” our sample.

The C+N abundances derived for the M5 subgiants show a large systematic increase in C+N as C decreases. To reproduce this requires the incorporation not only of CN, but of ON-processed material as well. Furthermore, the existence of this correlation is quite difficult to reproduce with an external mechanism such as “pollution” with material processed in a more massive AGB star, which mechanism is fundamentally stochastic in nature. We therefore suggest that although the internal mixing hypothesis has serious flaws, new theoretical insights are needed and it should not be ruled out yet.

The entire Keck/HIRES and LRIS user communities owes a huge debt to Jerry Nelson, Gerry Smith, Steve Vogt, Bev Oke, and many other people who have worked to make the Keck Telescope and HIRES and LRIS a reality and to operate and maintain the Keck Observatory. We are grateful to the W. M. Keck Foundation for the vision to fund the construction of the W. M. Keck Observatory. The authors wish to extend special thanks to those of Hawaiian ancestry on whose sacred mountain we are privileged to be guests. Without their generous hospitality, none of the observations presented herein would have been possible.

JGC acknowledges support from the National Science Foundation (under grant AST-9819614) and MMB acknowledges support from the National Science Foundation (under grant AST-0098489) and from the F. John Barlow endowed professorship. We are also in debt to Roger Bell for the use of the SSG program and the Dean of the UW Oshkosh College of Letters and Sciences for the workstation which made the extensive modeling possible.

This work has made use of the USNOFS Image and Catalog Archive operated by the United States Naval Observatory, Flagstaff Station (<http://www.nofs.navy.mil/data/fchpix/>).

REFERENCES

- Bell, R. A. & Gustafsson, B. 1978, A&AS, 34, 229
- Bell, R. A., Dickens, R. J. & Gustafsson, B., 1979, ApJ, 229, 604
- Bell, R. A., Hesser, J. E. & Cannon, R. D., 1983, ApJ, 269, 580
- Bell, R. A. & Gustafsson, B. 1989, MNRAS, 236, 653
- Bell, R. A., Briley, M. M., & Smith, G. H. 1990, AJ, 100, 187
- Bell, R. A., Paltoglou, G., & Tripicco, M. J. 1994, MNRAS, 268, 771
- Bellman, S., Briley, M.M., Smith, G.H. & Claver, C.F., 2001, PASP, 113, 326
- Bergbusch, P. A. & Vandenberg, D. A. 1992, ApJS, 81, 163
- Bono, G., Cassisi, S., Zoccali, M. & Piotto, G., 2001, ApJ, 546, L109
- Briley, M. M., Hesser, J. E. & Bell, R. A., 1991, ApJ, 373, 482
- Briley, M. M., Smith, G. H., Bell, R. A., Oke, J. B. & Hesser, J. E., 1992, ApJ, 387, 612
- Briley, M. M. & Smith, G. H. 1993, PASP, 105, 1260
- Briley, M. M., Hesser, J. E., Bolte, M. & Smith, G.H., 1994, AJ, 108, 2183
- Briley, M. M., Smith, V. V., Suntzeff, N. B., Lambert, D. L., Bell, R. A. & Hesser, J. E., 1996, Nature, 383, 604
- Briley, M. M., Smith, V. V., King, J., & Lambert, D. L. 1997, AJ, 113, 306
- Briley, M. M. & Cohen, J. G. 2001, AJ, 122, 242
- Briley, M. M., Smith, G. H. & Claver, C. F., 2001, AJ, 122, 2561
- Brown, J. E., Wallerstein, G. & Oke, J. B., 1990, AJ, 1561
- Cannon, R.D., Croke, B.F.W., Bell, R.A., Hesser, J.E. & Stathakis, R.A., 1998, MNRAS, 298, 601
- Carbon, D.F., Langer, G.E., Butler, D., Kraft, R., Suntzeff, N., Kemper, E., Trefzger, C. & Romanishin, W., 1982, ApJS, 49, 207
- Cavallo, R. M., Sweigart, A. V., & Bell, R. A., 1998, ApJ, 492, 575
- Charbonnel, C., 1994, A&A, 282, 811
- Charbonnel, C., 1995, ApJ, 453, L4

- Cohen, J. G., 1999, AJ, 117, 2434
- Cohen, J. G. & Cromer, J.L., 1988, PASP, 100, 1582
- D’Antona, F., Chieffi, A. & Gratton, R., 1983, Mem. S.A.It.,54, 129
- Denissenkov, P. A. & Denissenkova, S. N., 1990, SvAL, 16, 275
- Denissenkov, P. A. & Weiss, A., 1996, A&A, 308, 773
- Denissenkov, P. A. & Weiss, A., 2001, ApJ, 559, 115L
- Do Nascimento Jr., J. D., Charbonnel, C., Lèbre, A., de Laverny, P. & De Medeiros, J. R., 2000, A&A, 357, 931
- Gratton, R.G., Sneden, C., Carretta, E. & Bragaglia, A., 2000, A&A, 354, 169
- Gratton, R. G. *et al.*, 2001, A&A, 369, 87
- Gustafsson, B., Bell, R. A., Eriksson, K., & Nordlund, Å. 1975, A&A, 42, 407
- Gustafsson, B. & Bell, R. A. 1979, A&A, 74, 313
- Harris, W. E. 1996, AJ, 112, 1487
- Hesser, J. E., 1978, ApJ, 223, L117
- Hesser, J. E. & Bell, R. A., 1980, ApJ, 238, L149
- Houdashelt, M. L., Bell, R. A. & Sweigart, A. V., 2000, AJ, 119, 1448
- Iben, I. Jr. & Renzini, A., 1983, ARA&A, 21, 271
- Ivans, I. I., Kraft, R. P., Sneden, C., Smith, G. H., Rich, R. M., & Shetrone, M. 2001, AJ, 122, 1438
- Johnson, K. A. & Bolte, M., 1998, AJ, 115, 693
- Kraft, R. P. 1994, PASP, 106, 553
- Landolt, A. R., 1992, AJ, 104, 340
- Langer, G. E., 1985, PASP, 97, 382
- Langer, G. E., Kraft, R. P. & Friel, E. D., 1985, PASP, 97, 373
- Langer, G. E., Kraft, R.P., Carbon, D.F., Friel, E. & Oke, J.B., 1986, PASP, 98, 473
- Lattanzio, J., Charbonnel, C. & Forestini, M., 1999, in *The Changes in Abundances in AGB Stars*, (astro-ph/9912298)

- Meléndez, J., Barbuy, B., & Spite, F., 2001, ApJ, 556, 858
- Monet, D.G. *et al.*, 1998, USNO-A2.0 Catalog (on CD-ROM) (Flagstaff:USNO)
- Norris, J.E., Freeman, K.C. & DaCosta, G.S., 1984, ApJ, 277, 615
- Oke, J. B., Cohen, J. G., Carr, M., Cromer, J., Dingizian, A., Harris, F. H., Labrecque, S., Lucinio, R., Schaal, W., Epps, H., & Miller, J., 1995, PASP, 107, 307
- Pinsonneault, M., 1997, ARA&A, 35, 557
- Pryor, C. & Meylan, G., 1993, in *Structure and Dynamics of Globular Clusters*, ed. S. Djorgovski & G. Meylan, ASP, pg. 357
- Ramírez, S. V. & Cohen, J. G., AJ, (submitted)
- Sandquist, E. L., Bolte, M., Stetson, P. B., Hesser, J. E., 1996, ApJ, 470, 910
- Shetrone, M. D., Sneden, C. & Pilachowski, C. A., 1993, PASP, 105, 337
- Shortridge, K. 1988, “The Figaro Manual Version 2.4”
- Smith, G.H. & Norris, J., 1983, ApJ, 264, 215
- Smith, G.H., Shetrone, M.D., Bell, R.A., Churchill, C.W. & Briley, M.M., 1996, AJ, 112, 1511
- Smith, G. H., Shetrone, M. D., Briley, M. M., Churchill, C. W., & Bell, R. A. 1997, PASP, 109, 236
- Sneden, C., Kraft, R. P., Prosser, C. F., & Langer, G. E. 1992, AJ, 104, 2121
- Stetson, P.B., Hesser, J.E. & Smecker-Hane, T., 1998, PASP, 110, 533
- Stetson, P. B., Bolte, M., Harris, W. E., Hesser, J. E., van den Bergh, S., Vandenberg, D. A., Bell, R. A., Johnson, J. A., Bond, H. E., Fullton, L. K., Fahlman, G. C. & Richer, H. B., 1999, AJ, 117, 247
- Stetson, P.B., 2000, PASP, 112, 925
- Suntzeff, N. B., 1981, ApJS, 47, 1
- Suntzeff, N. B. & Smith, V. V. 1991, ApJ, 381, 160
- Sweigart, A. V. & Mengel, J. G., 1979, ApJ, 229, 624
- Trefzger, C.F., Carbon, D.F., Langer, G.E., Suntzeff, N.B. & Kraft, R.P., 1983, ApJ, 266, 144
- Tripicco, M. J. & Bell, R. A., 1995, AJ, 110, 3035
- Ventura, P., D’Antona, F., Mazzitelli, I., & Gratton, R. 2001, ApJ, 550, L65

Weiss, A., Denissenkov, P. A., & Charbonnel, C., 2000, *A&A*, 356, 181

Zoccali, M., Cassisi, G., Piotto, G., Bono, G. & Salaris, M., 1999, *ApJ*, 518, L49

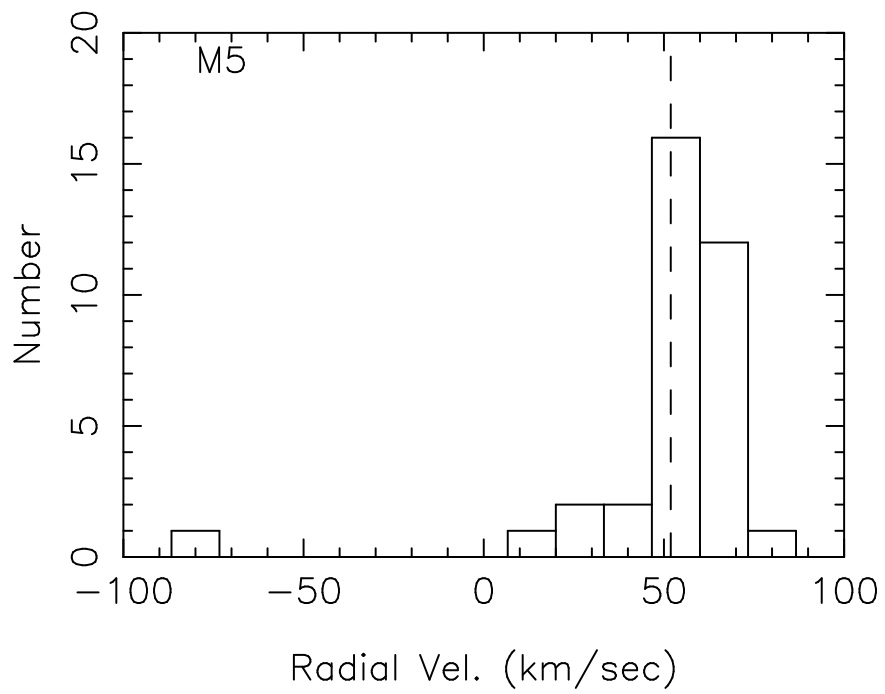


Fig. 1.— The histogram of the measured heliocentric radial velocities for approximately half of the sample stars in M5 is shown. The cluster v_r of Pryor & Meylan (1993) ($+51.9 \text{ km s}^{-1}$) is indicated as a dashed vertical line.

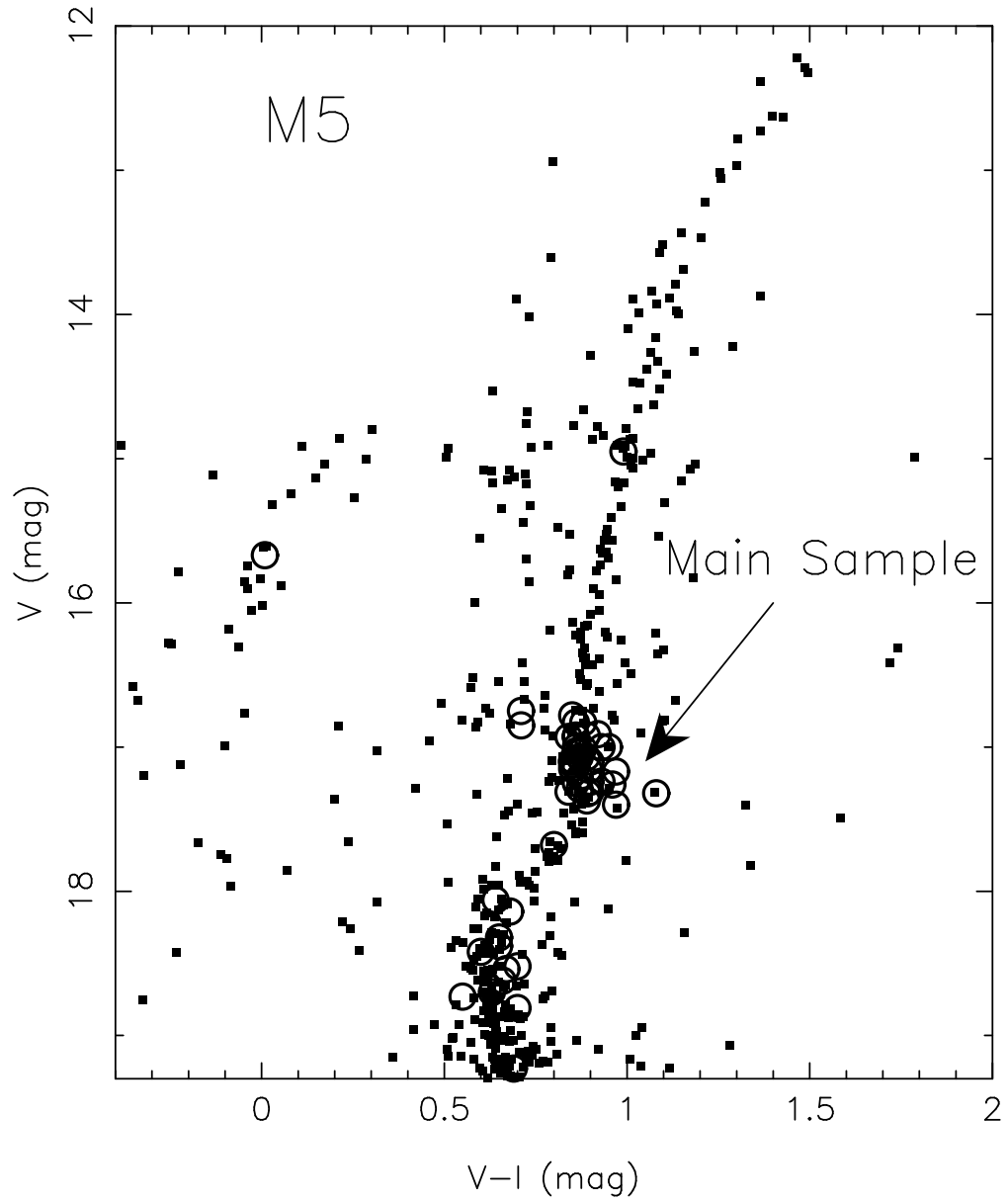


Fig. 2.— The primary sample of probable members of M5 at the base of the red giant branch used here is shown together with the secondary sample superposed on the (V, I) CMD diagram.

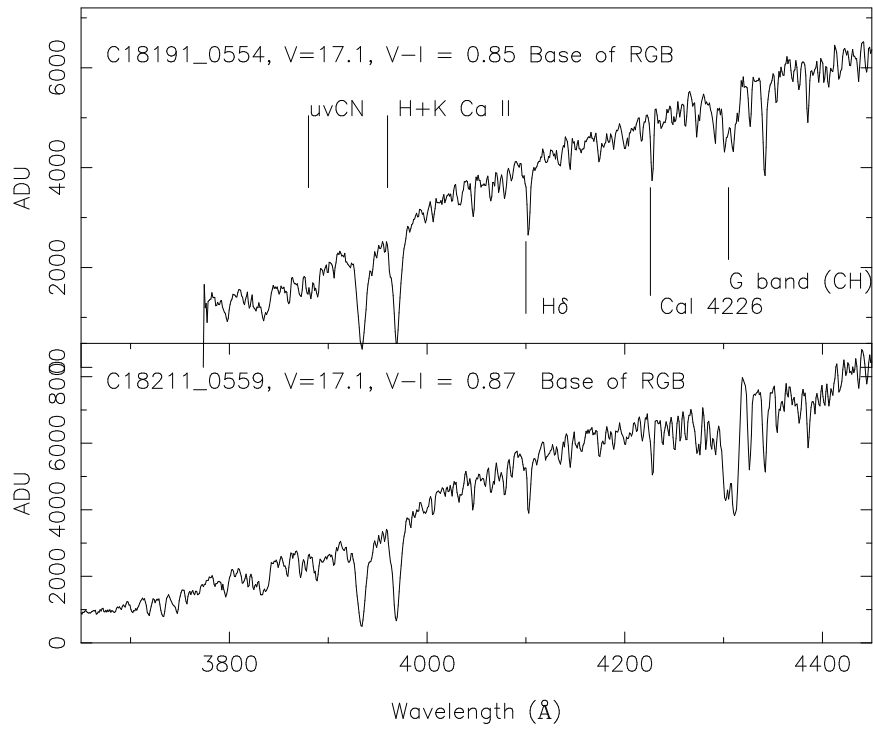


Fig. 3.— Part of the LRIS-B spectra of two probable members of M5. The stars are essentially identical in V mag and $V - I$ colors and are both located at the base of the subgiant branch. Note the difference in the strength of the G band of CH in these two spectra.

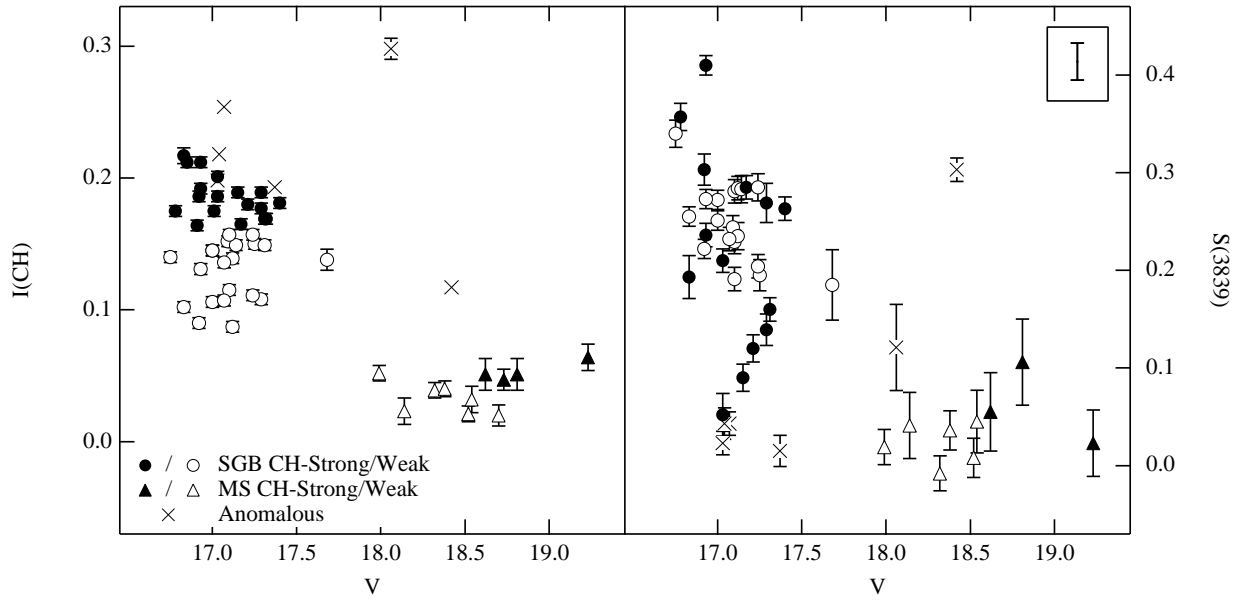


Fig. 4.— The measured I(CH) and S(3839) indices are plotted for the program stars as a function of V . The sample has been arbitrarily divided into two groups: CH-strong (filled markers) and CH-weak (open). Large and significant star-to-star differences exist in both CH and CN band strengths among the SGB stars. The decreasing spread in indices with luminosity is the result of increasing temperatures near the main sequence turn off. The error bar shown in the upper-right box represents the uncertainty in determining the slope of the uv continuum as described in §4.

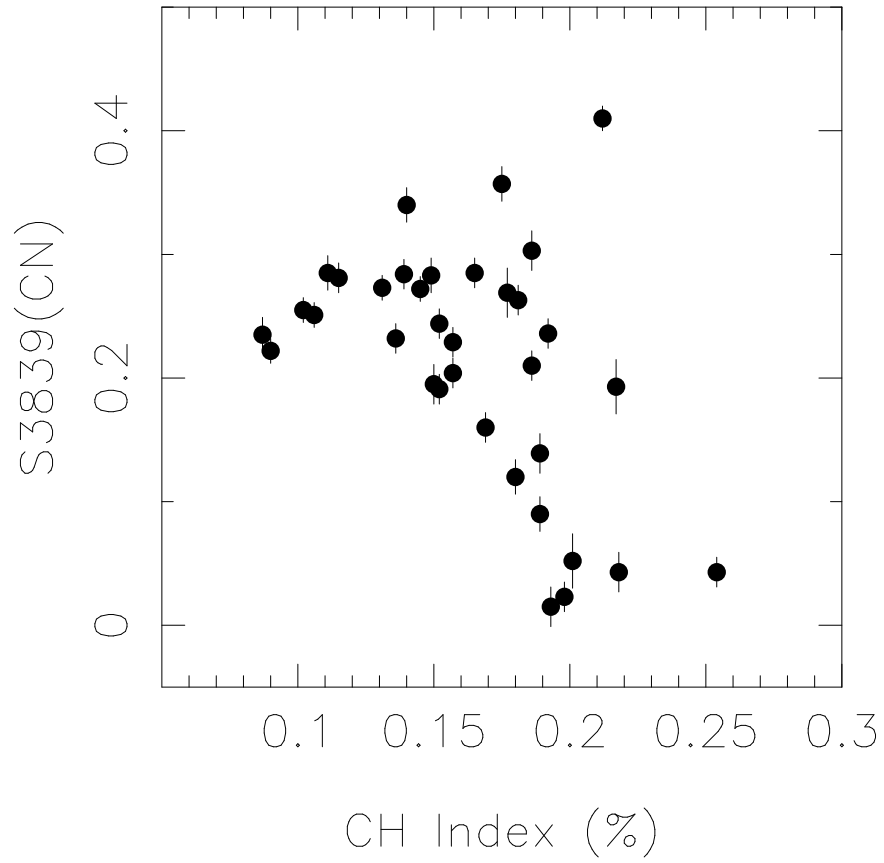


Fig. 5.— The CH and uvCN band indices are plotted against each other for the 43 stars with $16.5 < V < 17.5$ mag at the base of the RGB in M5. The two stars with the strongest CH indices were classified as anomalous.

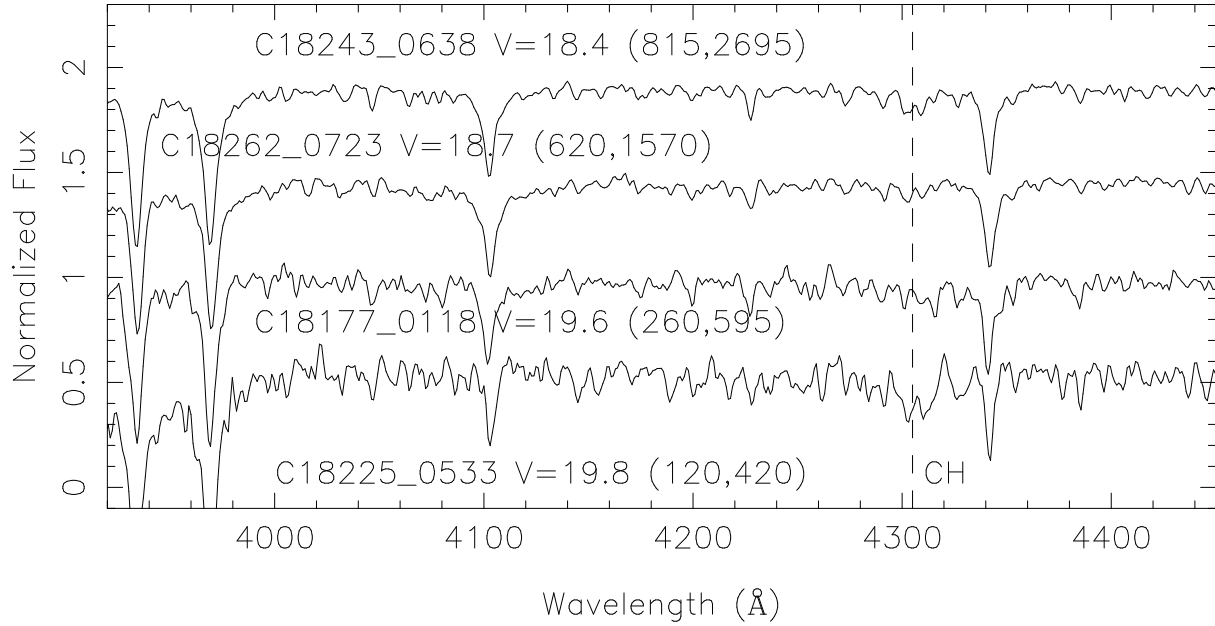


Fig. 6.— The region of the G band of CH in four main sequence stars in M5 going from top to bottom in order of increasing V mag. A constant arbitrary vertical offset between the spectra has been imposed for clarity. The label for each object gives in parentheses the DN/pixel at the blue and red end respectively in the original spectrum so that the signal-to-noise ratio can be calculated. The spectra have been slightly smoothed, then a continuum was fit from 3900 to 4500 Å, and the spectra were normalized. In addition to looking at the strength of the CH band, note that the strongest atomic features, particularly the Ca I lines at 4226Å and the Fe I lines at 4046 and 4384 Å, are also becoming stronger as T_{eff} decreases.

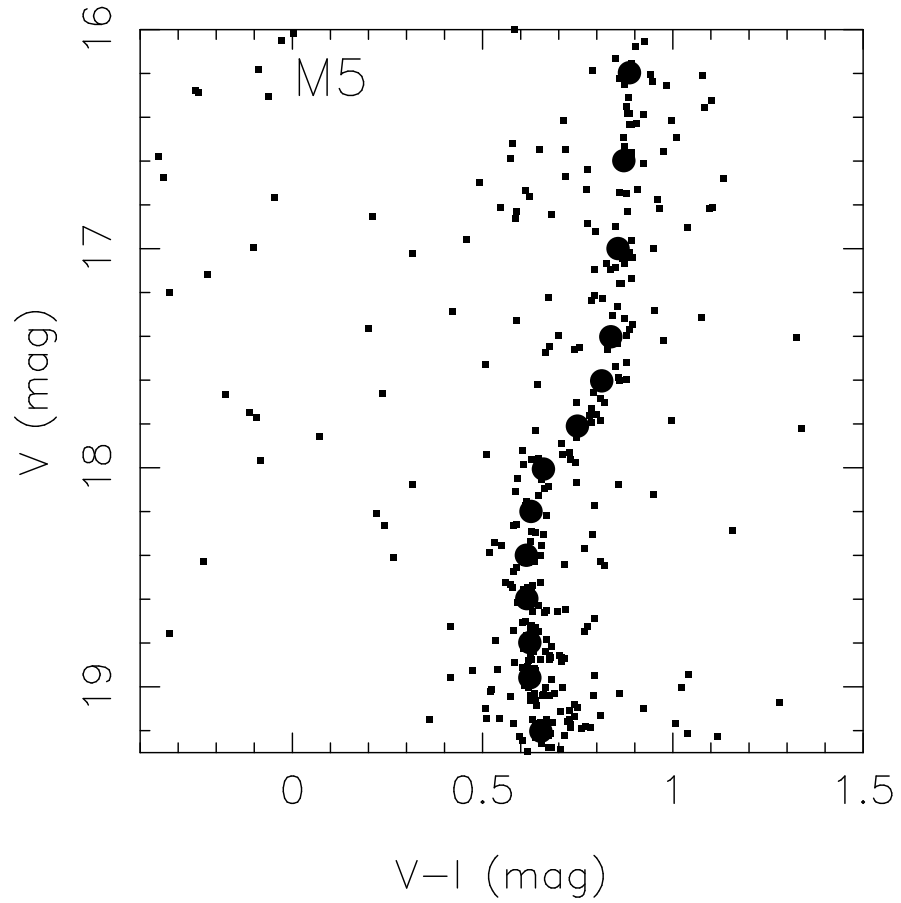


Fig. 7.— The model points for the grid of stellar atmospheres and spectral syntheses obtained from the isochrone are shown superposed on the (V, I) CMD diagram of M5 in the region of the subgiant branch and the upper main sequence.

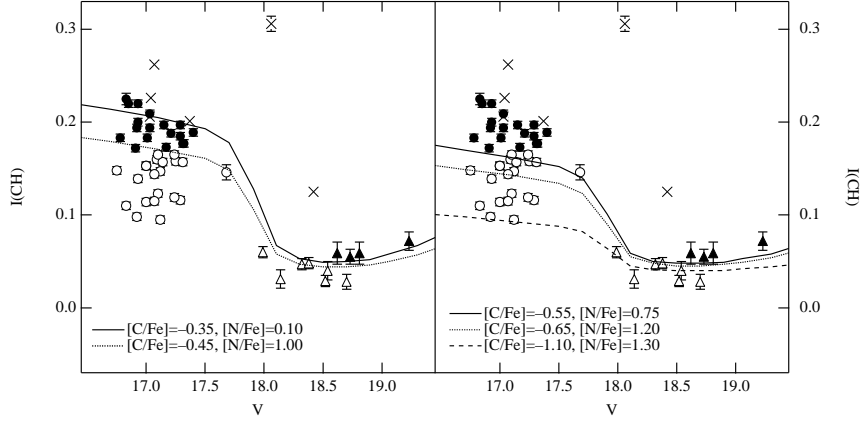


Fig. 8.— The observed $I(\text{CH})$ indices are plotted with calculated band strengths for several differing C (and N) abundances as listed in Table 4 as a function of V magnitude. As in Figure 4, the stars have been divided into two groups based on CH-band strength. Note that the range of CN-band strengths observed requires nearly a 0.75 dex star-to-star variation in $[\text{C}/\text{Fe}]$ among the SGB stars.

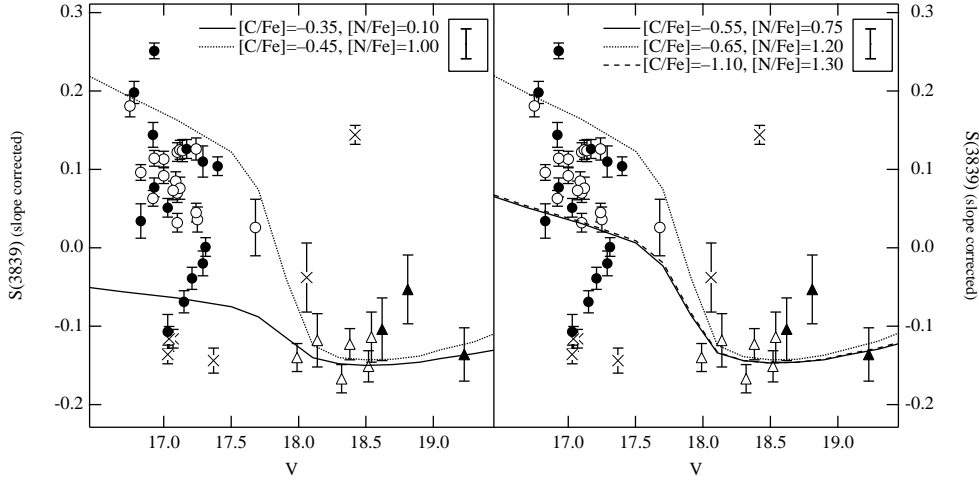


Fig. 9.— Observed $S(3839)$ indices are plotted with the model indices from Table 4 against V magnitude. As with Figure 8, a significant spread in abundances is present to within 0.5 mags of the MSTO. Among the MSTO stars themselves, the higher temperatures have resulted in CN band strengths too weak to measure accurately in the present spectra. The error bar shown in the boxes indicates the uncertainty in the $S(3839)$ offset due to the slope of the uv continuum (see §4).

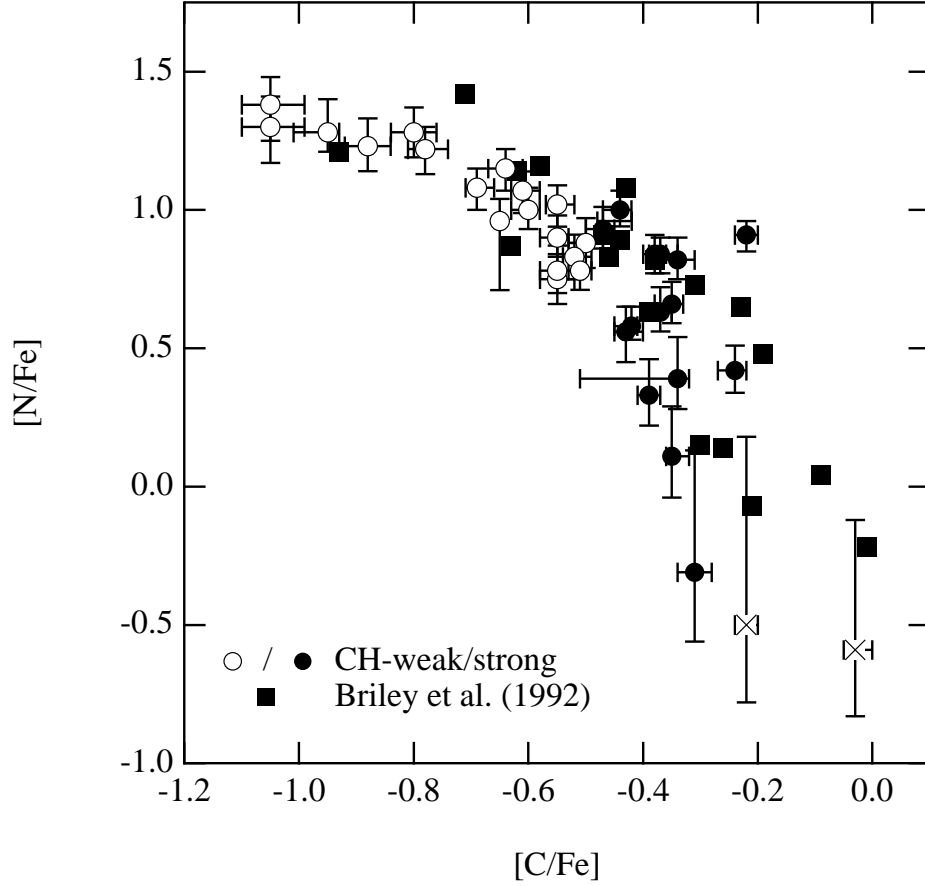


Fig. 10.— The resulting $[C/Fe]$ and $[N/Fe]$ abundances for the M5 SGB stars in Table 3 are plotted. A strong C versus N anti-correlation is evident which also compares well with the relation from Briley *et al.* (1992) among a sample of more luminous cluster members (plotted as filled squares). The presence of such an anticorrelation, although suggestive of the presence of atmospheric material exposed to the CN-cycle, is difficult to explain via internal processes given the evolutionary state of the present sample of stars.

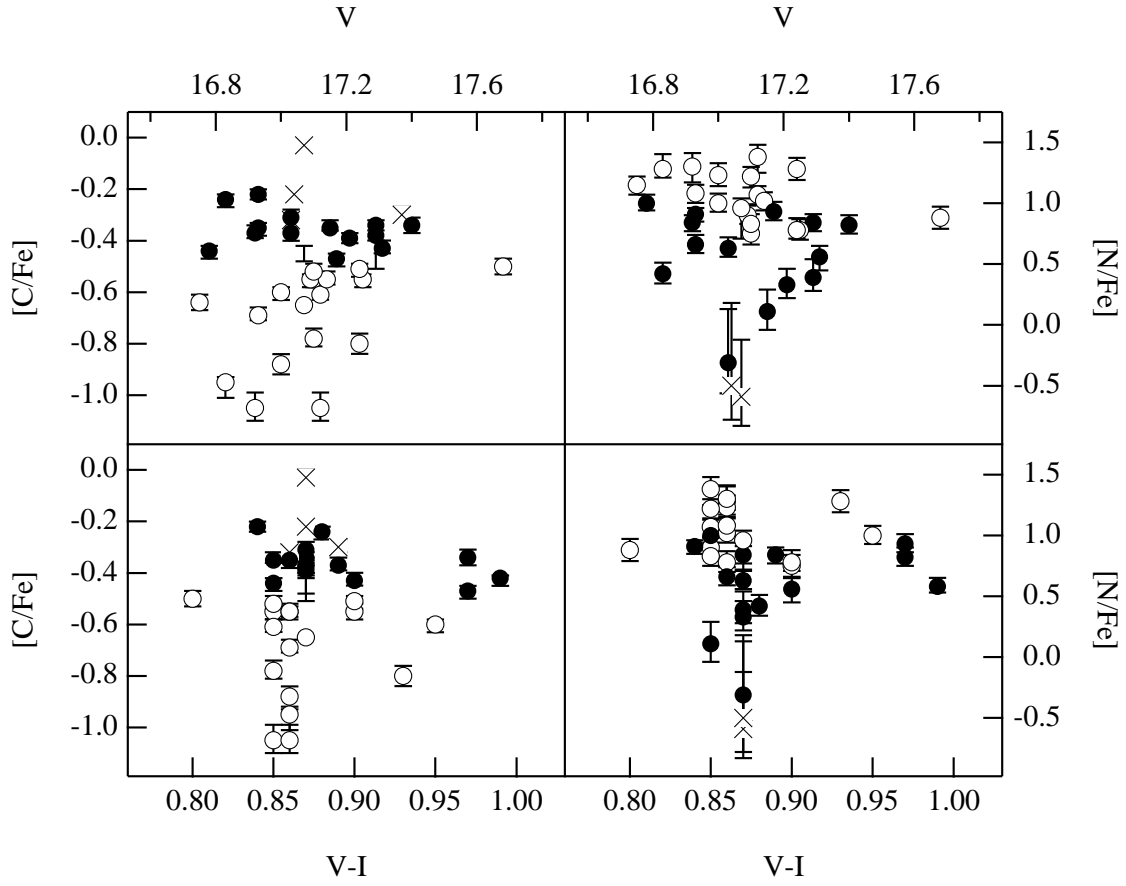


Fig. 11.— The derived C and N abundances are plotted against photometry for the SGB stars of Table 3. No systematic trends with either luminosity or temperature are apparent in the abundances.

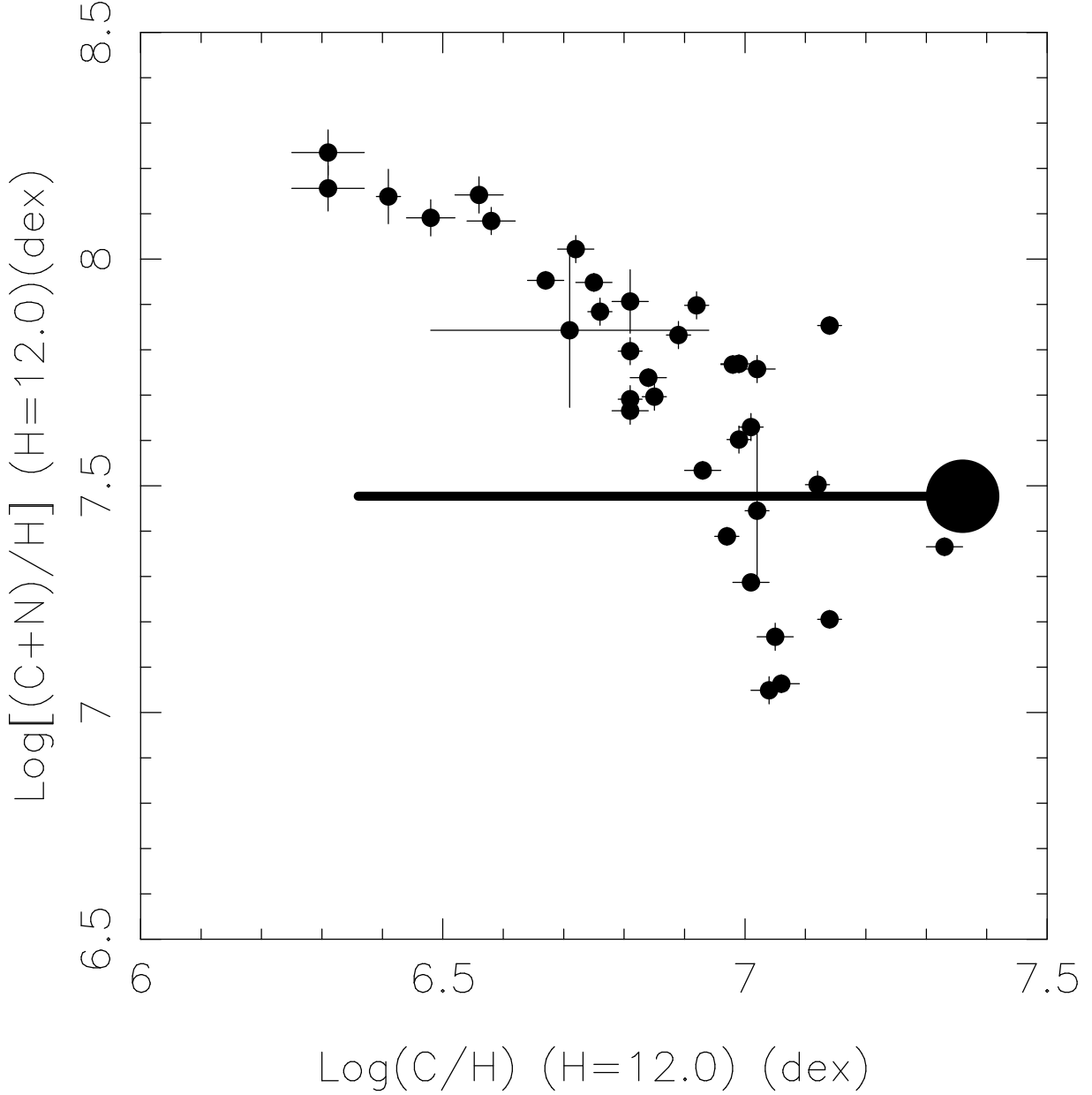


Fig. 12.— The sum of the derived C and N abundances is plotted as a function of the C abundance. The large filled circle marks the location for both C and N depleted by a factor of 16, adopting the abundance of M5 of $[\text{Fe}/\text{H}] = -1.2$ dex, with C/N at the Solar ratio. The horizontal line extending to the left of that represents the locus of points for C gradually being converted into N, with the left end of the line having $\text{C}/\text{C}_0 = 0.1$.

Table 1. Probable Non-Members of M5

ID	Sample (P or S)	v_r (km s ⁻¹)	Abs. Spectrum	$\Delta[V, I]^a$ (mag)
Non-members:				
C18262_0726	P	-73.1	Metal rich	+0.03
C18465_0208	P	... ^b	Metal rich	+0.21
Probable Members:				
C18285_0147	P	+60.7	OK	+0.14
C18408_0805	P	... ^b	OK	-0.14
C18488_0120	P	... ^b	OK	-0.14
Uncertain:				
C18383_0722 ^c	S	... ^b	BHB ?	-0.16

^aThis is $[V - I \text{ for the star}] - [V - I \text{ for the cluster locus}]$ evaluated at the V mag of the star.

^bNo radial velocity is available for this star.

^cThis faint star is possibly a blue straggler in M5 or possibly a background early-type star.

Table 2. Photometry for Members of M5 in Our Sample

ID ^a	<i>B</i> (mag)	<i>V</i> (mag)	<i>I</i> (mag)
C18149_0401	17.66	16.93	16.07
C18159_0608	17.79	17.10	16.25
C18174_0329	15.80	14.95	13.96
C18175_0332	17.63	16.93	16.07
C18177_0109	17.76	17.10	16.20
C18177_0118	20.00	19.56	18.81
C18177_0123	18.04	17.37	16.48
C18181_0205	17.89	17.24	16.34
C18182_0207	19.17	18.81	18.11
C18184_0442	17.68	17.00	16.14
C18187_0216	17.94	17.31	16.41
C18191_0554	17.81	17.12	16.27
C18195_0301	17.77	17.07	16.20
C18200_0241	17.92	17.21	16.32
C18200_0251	18.97	18.54	17.87
C18200_0351	17.84	17.15	16.30
C18204_0418	17.52	16.83	15.97
C18204_0524	17.78	17.09	16.24
C18204_0521	18.34	17.68	16.88
C18206_0733	18.88	18.42	17.82
C18211_0559	18.59	18.06	17.42
C18225_0533	20.41	19.83	19.08
C18225_0537	17.79	17.07	16.20
C18240_0320	17.54	16.92	16.06
C18240_0621	17.65	16.93	16.09
C18240_0705	17.71	17.03	16.17
C18241_0216	17.63	17.00	16.05
C18243_0634	17.78	17.16	16.26
C18243_0638	18.87	18.38	17.73
C18246_0716	17.72	17.03	16.16
C18257_0756	18.00	17.31	16.47
C18262_0723	19.19	18.70	18.07
C18285_0147	17.82	17.32	16.24
C18268_0132	17.73	17.07	16.18
C18384_0725	17.50	16.78	15.95

Table 2—Continued

ID ^a	<i>B</i> (mag)	<i>V</i> (mag)	<i>I</i> (mag)
C18384_0728	18.58	18.14	17.46
C18386_0709	17.60	16.92	16.03
C18408_0805	17.62	16.75	16.04
C18412_0233	17.78	17.17	16.20
C18413_0647	17.86	17.26	16.30
C18422_0256	18.89	18.52	17.82
C18422_0306	17.86	17.24	16.31
C18422_0318	19.73	(19.23) ^b	18.54
C18422_0748	18.58	18.14	17.46
C18422_0757	17.74	17.03	16.16
C18429_0337	18.00	17.40	16.43
C18437_0548	19.13	18.62	17.96
C18442_0658	17.93	17.25	16.39
C18448_0557	17.75	17.04	16.17
C18461_0520	17.96	17.32	16.43
C18478_0505	18.75	18.32	17.67
C18478_0508	17.79	17.10	16.25
C18484_0608	17.82	17.14	16.28
C18488_0120	17.79	16.85	16.14
C18496_0637	17.94	17.29	16.42
C18501_0410	19.38	18.73	18.18
C18502_0146	17.65	17.00	16.07
C18502_0405	17.57	16.91	15.99
C18502_0447	17.68	17.01	16.13
BHB Star			
C18386_0713	15.56	15.60	15.59

^aThe star names are derived from their J2000 coordinates. Star C12345_5432 has coordinates 15 12 34.5 +2 54 32 (J2000).

^bThe *V* mag is obtained from the *B*, *B* – *I* assuming the object is on the main sequence of M5, as suggested by the available *B*, *I* photometry.

Table 3. Indices, Model Parameters, and Resulting Abundances

Star	Comment	I(CH)	ϵ I(CH)	S(3839)	ϵ S(3839) ^a	T_{eff}	log g	[C/Fe]
C18149_0401	SGB-CH-Strong	0.192	0.004	0.236	0.012	5192	3.23	-0.35
C18159_0608	SGB-CH-Weak	0.157	0.004	0.229	0.012	5216	3.31	-0.52
C18174_0329	SGB-CH-Strong	0.221	0.004	0.346	0.012	4849	2.29	-0.42
C18175_0332	SGB-CH-Weak	0.131	0.004	0.273	0.010	5192	3.23	-0.69
C18177_0109	SGB-CH-Weak	0.152	0.004	0.191	0.012	5216	3.31	-0.55
C18177_0118	MS-CH-Weak	0.022	0.012	0.049	0.042	-	-	-
C18177_0123	Anomalous	0.193	0.004	0.015	0.016	5260	3.44	-0.30
C18181_0205	SGB-CH-Weak	0.157	0.004	0.204	0.012	5237	3.38	-0.51
C18182_0207	MS-CH-Strong	0.051	0.012	0.106	0.044	-	-	-
C18184_0442	SGB-CH-Weak	0.106	0.004	0.251	0.010	5202	3.26	-0.88
C18187_0216	SGB-CH-Strong	0.169	0.004	0.160	0.012	5249	3.41	-0.43
C18191_0554	SGB-CH-Weak	0.139	0.004	0.284	0.012	5219	3.32	-0.61
C18195_0301	SGB-CH-Weak	0.136	0.004	0.232	0.012	5212	3.30	-0.65
C18200_0241	SGB-CH-Strong	0.180	0.004	0.120	0.014	5232	3.36	-0.39
C18200_0251	MS-CH-Weak	0.032	0.010	0.045	0.032	-	-	-
C18200_0351	SGB-CH-Strong	0.189	0.004	0.090	0.014	5223	3.33	-0.35
C18204_0418	SGB-CH-Weak	0.102	0.004	0.255	0.010	5178	3.18	-0.95
C18204_0521	SGB-CH-Weak	0.138	0.008	0.185	0.036	5364	3.60	-0.50
C18204_0524	SGB-CH-Weak	0.152	0.004	0.244	0.012	5215	3.31	-0.55
C18206_0533	Anomalous - Strong CN/CH	0.117	0.004	0.303	0.012	-	-	-
C18211_0559	Anomalous - Strong CN/CH	0.298	0.008	0.121	0.044	-	-	-
C18225_0537	Anomalous	0.254	0.004	0.043	0.012	5212	3.30	-0.03
C18225_0533	MS-CH-Weak	0.085	0.014	-0.006	0.062	-	-	-
C18240_0320	SGB-CH-Weak	0.090	0.004	0.222	0.010	5190	3.22	-1.05
C18240_0621	SGB-CH-Strong	0.212	0.004	0.410	0.010	5192	3.23	-0.22
C18240_0705	Anomalous	0.198	0.004	0.023	0.012	5206	3.28	-0.32
C18241_0216	SGB-CH-Weak	0.145	0.004	0.272	0.010	5202	3.26	-0.60
C18243_0634	SGB-CH-Weak	0.087	0.004	0.235	0.014	5219	3.32	-1.05
C18243_0638	MS-CH-Weak	0.040	0.006	0.036	0.020	-	-	-
C18246_0716	SGB-CH-Strong	0.186	0.004	0.210	0.012	5206	3.28	-0.37
C18257_0756	SGB-CH-Weak	0.149	0.004	-	-	-	-	-
C18262_0723	MS-CH-Weak	0.020	0.008	-	-	-	-	-
C18268_0132	SGB-CH-Weak	0.107	0.004	-	-	-	-	-
C18285_0147	SGB-CH-Strong	0.169	0.004	-	-	-	-	-
C18384_0725	SGB-CH-Strong	0.175	0.004	0.357	0.014	5170	3.16	-0.44
C18384_0728	SGB-CH-Strong	0.217	0.006	0.193	0.022	5178	3.18	-0.24

Table 3—Continued

Star	Comment	I(CH)	ϵ I(CH)	S(3839)	ϵ S(3839) ^a	T_{eff}	log g	[C/Fe]	ϵ [C/Fe]
C18386_0709	SGB-CH-Strong	0.186	0.004	0.303	0.016	5190	3.22	-0.37	0.03
C18408_0805	SGB-CH-Weak	0.140	0.004	0.340	0.014	5166	3.14	-0.64	0.03
C18412_0233	SGB-CH-Strong	0.165	0.004	0.285	0.012	5226	3.34	-0.47	0.02
C18413_0647	SGB-CH-Strong	0.177	0.004	0.269	0.020	5245	3.40	-0.38	0.02
C18422_0256	MS-CH-Weak	0.021	0.006	0.008	0.020	-	-	-	-
C18422_0306	SGB-CH-Weak	0.111	0.004	0.285	0.014	5237	3.38	-0.80	0.04
C18422_0318	MS-CH-Weak	0.052	0.006	0.019	0.018	-	-	-	-
C18422_0748	MS-CH-Weak	0.023	0.010	0.041	0.034	-	-	-	-
C18422_0757	SGB-CH-Strong	0.201	0.004	0.052	0.022	5206	3.28	-0.31	0.03
C18429_0337	SGB-CH-Strong	0.181	0.004	0.263	0.012	5266	3.45	-0.34	0.03
C18437_0548	MS-CH-Strong	0.051	0.012	0.055	0.040	-	-	-	-
C18442_0658	SGB-CH-Weak	0.150	0.004	0.195	0.016	5239	3.38	-0.55	0.02
C18448_0557	Anomalous	0.218	0.004	0.043	0.016	5208	3.28	-0.22	0.02
C18461_0520	SGB-CH-Strong	0.189	0.004	0.139	0.016	5245	3.40	-0.34	0.02
C18478_0505	MS-CH-Weak	0.039	0.006	-0.008	0.018	-	-	-	-
C18478_0508	SGB-CH-Weak	0.115	0.004	0.281	0.012	5216	3.31	-0.78	0.04
C18484_0608	SGB-CH-Weak	0.149	0.004	0.283	0.014	5222	3.33	-0.55	0.03
C18488_0120	SGB-CH-Strong	0.212	0.004	-	-	-	-	-	-
C18496_0637	SGB-CH-Weak	0.108	0.004	-	-	-	-	-	-
C18501_0410	MS-CH-Strong	0.047	0.008	-	-	-	-	-	-
C18502_0146	SGB-CH-Weak	0.145	0.004	-	-	-	-	-	-
C18502_0405	SGB-CH-Strong	0.164	0.004	-	-	-	-	-	-
C18502_0447	SGB-CH-Strong	0.175	0.004	-	-	-	-	-	-

^aThe uncertainty in the zero point for S(3839) is not included in the values listed above, and is ± 0.019 .

Table 4. Model Parameters, Colors, and Resulting Indices

T_{eff}	$\log g$	M_V	$V - I$	[C/Fe]=-0.35, [N/Fe]=+0.10		[C/Fe]=-0.45, [N/Fe]=+1.0		[C/Fe]=-0.55, [N/Fe]=+1.0	
				I(CH)	S(3839)	I(CH)	S(3839)	I(CH)	S(3839)
5103	2.94	1.887	0.851	0.225	-0.001	0.189	0.278	0.175	0.278
5159	3.12	2.288	0.836	0.217	-0.010	0.182	0.243	0.167	0.243
5216	3.31	2.689	0.821	0.208	-0.018	0.174	0.209	0.159	0.209
5291	3.50	3.092	0.802	0.196	-0.029	0.164	0.168	0.149	0.168
5379	3.61	3.293	0.778	0.181	-0.042	0.151	0.120	0.137	0.120
5626	3.79	3.500	0.714	0.131	-0.069	0.109	0.006	0.098	0.006
5997	3.99	3.696	0.625	0.070	-0.094	0.061	-0.078	0.056	-0.078
6148	4.11	3.889	0.592	0.056	-0.102	0.050	-0.094	0.047	-0.094
6209	4.21	4.089	0.580	0.052	-0.104	0.047	-0.097	0.045	-0.097
6214	4.28	4.287	0.581	0.053	-0.103	0.047	-0.096	0.045	-0.096
6186	4.35	4.488	0.589	0.055	-0.100	0.049	-0.092	0.046	-0.092
6133	4.41	4.648	0.589	0.061	-0.095	0.053	-0.084	0.050	-0.084
6062	4.46	4.892	0.618	0.070	-0.089	0.060	-0.074	0.055	-0.074
5980	4.51	5.094	0.636	0.082	-0.083	0.069	-0.060	0.063	-0.060

Table 5. Changes in Derived C and N Abundances for Different Model Parameters

Star	$\Delta(m-M)_V = -0.10$		$[O/Fe] = +0.15$		$C^{12}/C^{13} = 4^a$		$[Fe/H] = -$		
	[C/Fe]	[N/Fe]	$\Delta[C/Fe]$	$\Delta[N/Fe]$	$\Delta[C/Fe]$	$\Delta[N/Fe]$	$\Delta[C/Fe]$	$\Delta[N/Fe]$	
C18200_0351	-0.36	0.13	0.01	0.01	0.03	0.01	0.00	-0.02	0.08
C18429_0337	-0.36	0.83	0.03	0.01	0.05	0.00	-0.08	0.06	0.09
C18243_0634	-1.08	1.41	0.03	0.00	0.04	0.01	0.01	-0.02	0.14

^aReduced from the adopted value of $C^{12}/C^{13} = 10$.